Contemporary Physics, 1997, volume 38, number 3, pages 205 – 241

From snowflake formation to growth of bacterial colonies II: Cooperative formation of complex colonial patterns

ESHEL BEN-JACOB

In nature, bacterial colonies must often cope with hostile environmental conditions. To do so they have developed sophisticated cooperative behaviour and intricate communication capabilities, such as direct cell – cell physical interactions via extra-membrane polymers, collective production of extracellular 'wetting' fluid for movement on hard surfaces, long-range chemical signalling such as quorum sensing and chemotactic (bias of movement according to gradient of chemical agent) signalling, collective activation and deactivation of genes and even exchange of genetic material. Utilizing these capabilities, the bacterial colonies develop complex spatio-temporal patterns in response to adverse growth conditions. We present a wealth of beautiful patterns formed during colonial development of various bacterial strains and for different environmental conditions. Invoking ideas from pattern formation in non-living systems and using generic modelling we are able to reveal novel bacterial strategies which account for the salient features of the evolved patterns. Using the models, we demonstrate how bacterial communication leads to colonial self-organization that can only be achieved via cooperative behaviour of the cells. It can be viewed as the action of a singular feedback between the microscopic level (the individual cells) and the macroscopic level (the colony) in the determination of the emerging patterns.

1. Introduction

Among evolving (non-equilibrium) systems, living organisms are the most challenging that scientists can study. A biological system constantly exchanges material and energy with the environment as it regulates its growth and survival. The energy and chemical balances at the cellular level involve an intricate interplay between the microscopic dynamics and the macroscopic environment, through which life at the intermediate mesoscopic scale is maintained [1]. The development of a multicellular structure requires non-equilibrium dynamics, as microscopic imbalances are translated into the macroscopic gradients that control collective action and growth [2].

Much effort has been devoted to the search for basic principles of growth (communication, regulation and control) on the cellular and multicellular levels [3 – 10].

Armed with the new developments in the study of patterning in non-living systems, I set out to meet the challenge posed by living organisms. Of extreme importance was the choice of starting point, that is which phenomena to study; it had to be simple enough to allow progress but also well motivated by the significance of the results. In addition, I wanted to be able to use my previous knowledge and expertise. Cooperative microbial behaviour was well suited to my requirements.

1.1. *Complex bacterial patterns*

Traditionally, bacterial colonies are grown on substrates with a high nutrient level and intermediate agar concentration. Such 'friendly' conditions yield colonies of simple compact patterns, which fit well the contemporary view of bacterial colonies as a collection of independent unicellular organisms (non-interacting 'particles'). However, bacterial colonies in nature must regularly cope with hostile environmental conditions [5, 11]. Expecting complex patterns to be developed by stressed colonies, we created hostile conditions in a Petri dish by using a very low level of nutrients, a hard surface (high concentration of agar), or both.

Indeed, we observed some very complex patterns (figure 1). Drawing on the analogy with diffusive patterning in non-living systems [12 – 15], we can say that complex patterns are expected. The cellular reproduction rate that

Author's address: School of Physics and Astronomy, Raymond and Beverly Sackler Faculty of Exact Sciences, Tel-Aviv University, Tel-Aviv 69978, Israel.

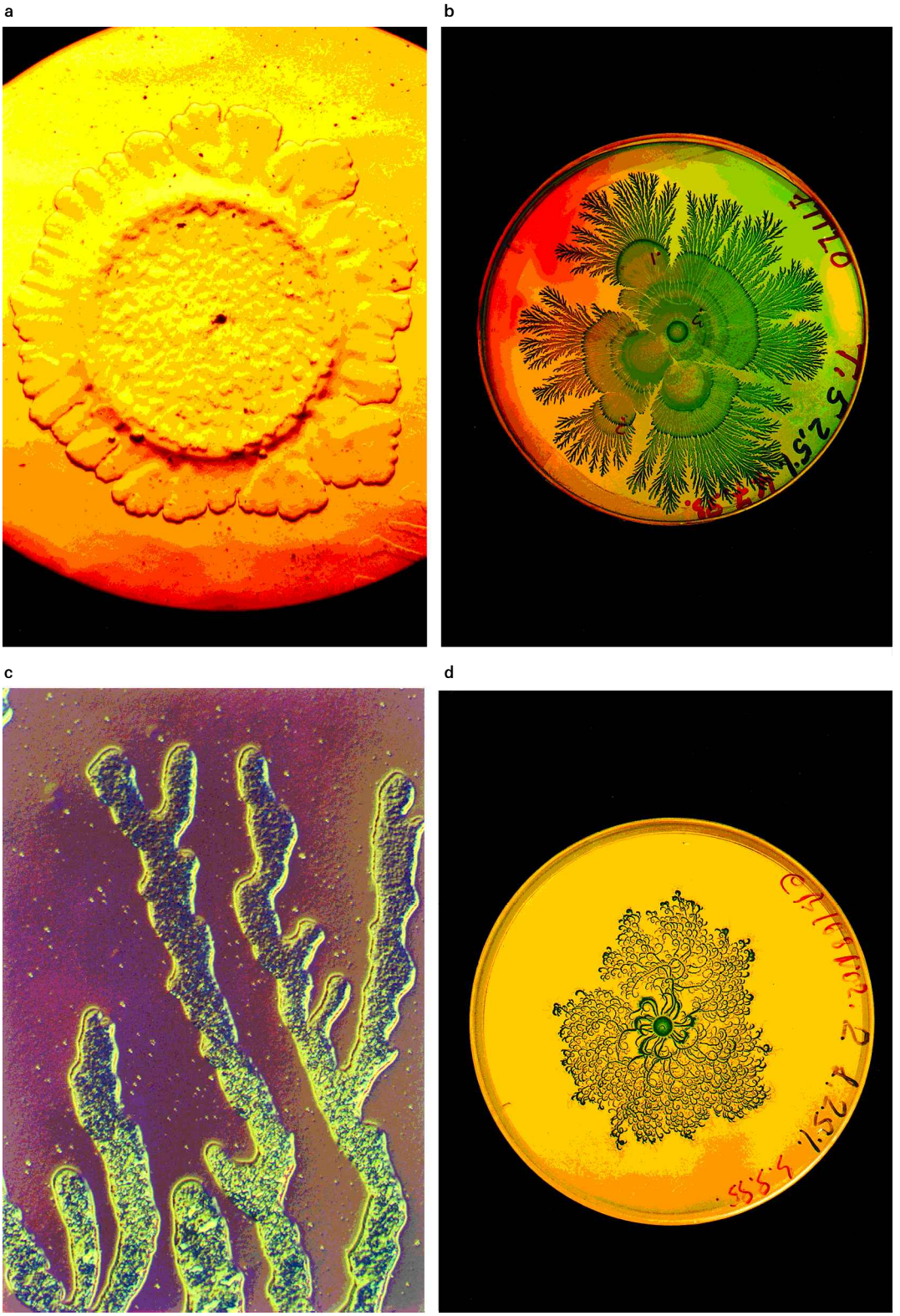

Figure 1. Examples of the observed complex patterns. (*a*) A colony of *B. subtilis* 168 grown at a peptone level of 2 g l^{-1} and an agar concentration of 1.5% . The pattern is compact with rough interface. (*b*) Branching pattern of the $\mathcal{T}$ morphotype grown at a peptone level of 5 g l^{-1} and an agar concentration of 2.5% . (*c*) Closer look at the branches with a magnification of 50 × and using the Nomarski method (polarized light) to show the height of the branches and their envelope. (*d*), (*e*) Examples of chiral patterns developed by colonies of

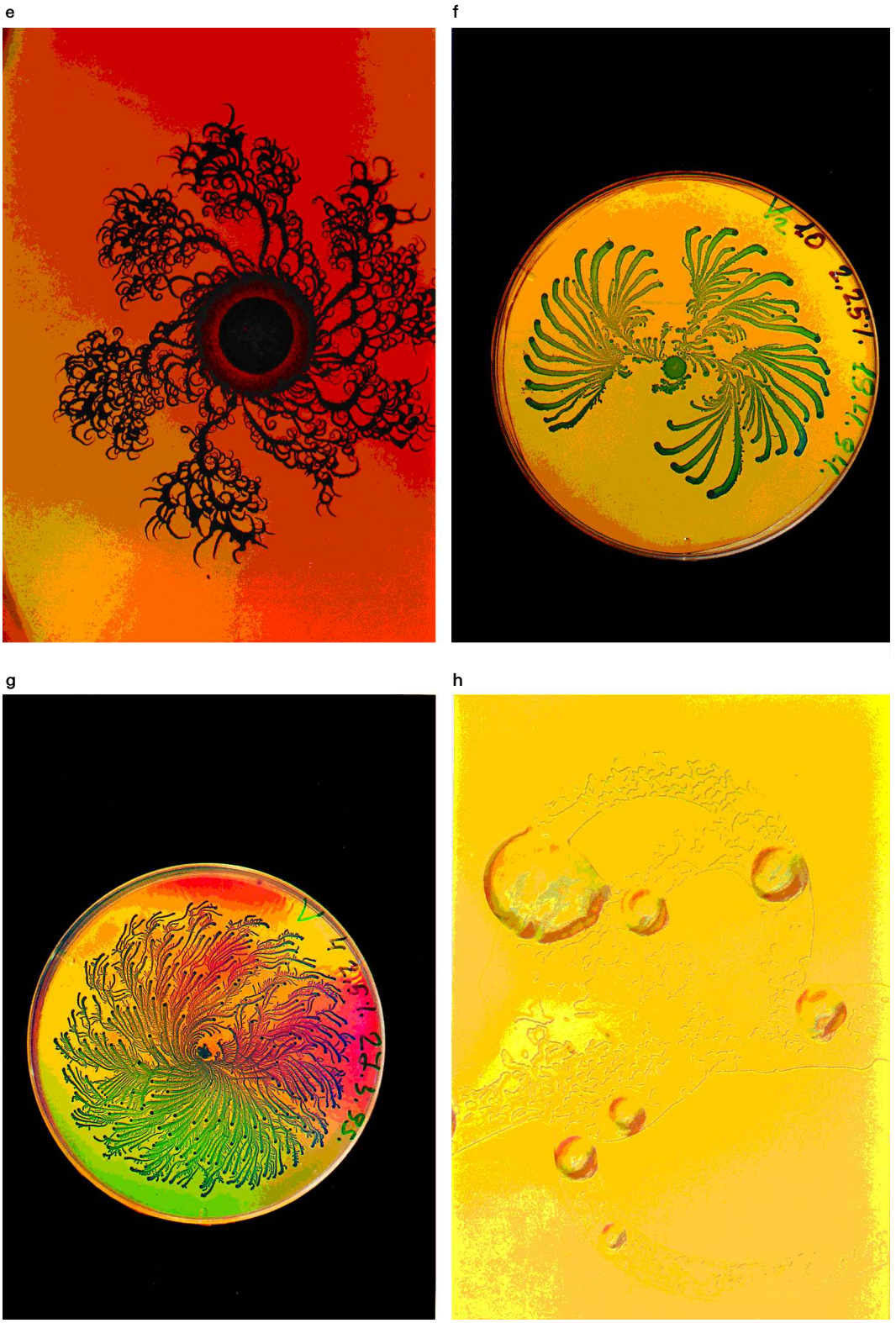

the *C* morphotype. Note that all the branches have a twist with the same handedness. (*f*) and (*g*) Examples of patterns developed by colonies of the *Y* morphotype. Each of the dots at the tips of the branches is made of many bacterial cells, all circulating the centre of the dot to form a vortex. (*h*) An optical microscope view (a magnification of 50 × and using the Nomarski method) of the vortices.

determines the growth rate of the colony is limited by the level of nutrients available for the cells. The latter is limited by the diffusion of nutrients towards the colony (for low-nutrient substrate). Hence the colonial growth should be similar to diffusion-limited growth in non-living systems, such as solidification from a supersaturated solution, invasion of viscous fluid by a less viscous one (Hele–Shaw system) or electrochemical deposition [14, 15]. The study of diffusive patterning in non-living systems teaches us that the diffusion field drives the system towards decorated (on many length scales) irregular fractal shapes [16, 17]. Indeed, bacterial colonies can develop patterns reminiscent of those observed during growth in non-living systems [18–26]. However, one should not conclude that complex patterning of bacterial colonies is yet another example (albeit more involved) of spontaneous emergence of patterns that may be explained according to the theory of patterning in non-living systems.

Bacterial colonies exhibit richer behaviour than patterning of non-living systems, reflecting the additional levels of complexity involved [22, 23, 27–32]. The building blocks of the colonies are themselves living systems, each having its own autonomous self-interest and internal degrees of freedom. At the same time, efficient adaptation of the colony to adverse growth conditions requires self-organization on all levels, which can only be achieved via cooperative behaviour of the individual cells. It may be viewed as the action of singular interplay [22–24] between the microscopic level (the individual cell) and the macroscopic level (the colony) in the determination of the emerging pattern. In general, as growth conditions worsen, more complex global structures are observed along with more sophisticated strategies of cooperation.

To achieve the required level of cooperation, the bacteria have developed various communication capabilities, such as firstly direct cell–cell physical and chemical interactions [33, 34], secondly indirect physical and chemical interactions, for example production of extracellular 'wetting' fluid [35, 36], thirdly long-range chemical signalling, such as quorum sensing [37, 38], and fourthly chemotactic response to chemical agents which are emitted by the cells [39–41] (see section 3 for definition of chemotaxis).

The communication capabilities enable each bacterial cell to be both an actor and a spectator (using Bohr's expressions) during the complex patterning. The bacteria developed a kind of particle–field duality; each of the cells is a localized (moving) particle that can produce chemical and physical fields around itself. For researchers in the pattern formation field, the above communication, regulation and control mechanisms open a new class of tantalizing complex models exhibiting a much richer spectrum of patterns than the models of azoic (non-living) systems.

Looking at the colonies, it becomes evident that we should view them as adaptive cybernetic systems or multicellular organisms which possess fantastic capabilities to cope with hostile environmental conditions and survive them (in contrast with the contemporary view of the colony as a collection of non-interacting passive 'particles').

1.2. *Birth of new morphotypes*

Motivated by observations of fractal colony patterns [18, 19, 42] and the developments in adaptive (directed) mutagenesis [43–50], I set up new experiments with a special goal in mind. The idea was to use conditions of diffusion-limited growth as an external pressure that will lead to a directed mutation toward motility on a hard agar surface. My working hypothesis was that mutations are expected from a strain which expands slowly (non-motile) into a faster strain (motile), that is one whose colony can propagate more rapidly on the agar surface; so it has an advantage in reaching the food.

We started our endeavour with *Bacillus subtilis* 168 which is non-motile on agar surface but is motile in fluids or inside very soft agar. We performed numerous experiments in which colonies of *B. subtilis* were grown under conditions of low nutrient (a peptone level of about $1\ g\ l^{-1}$) and mild agar (about 1.5% agar concentration). Occasionally, bursts of a new mode of growth exhibiting branching patterns were observed [22, 28]. This new mode of tip-splitting growth was found to be inheritable and transferable by a single cell [22, 23]; hence it is referred to as a distinctive morphotype as suggested by Gutnick [51]. To indicate the tip-splitting character of the growth it is denoted the $\mathcal{T}$ morphotype.

Microscopic observations reveal that the bacterial cells of $\mathcal{T}$ morphotype are indeed motile on the agar surface as we expected. Changes in motility on surfaces, both phenotypic and genotypic, are known in bacteria [52]; so at first the 'birth' of this new morphotype was not too surprising. Later, together with microbiologist collaborators, we performed genetic studies on the $\mathcal{T}$ morphotype and found it to differ from the original *B. subtilis* 168 [23]. The genetic identity of the $\mathcal{T}$ morphotype, its relation to *B. subtilis* 168 and its origin are currently under investigation [53].

In figure 1 we also show patterns developed by two additional distinct morphotypes. One is characterized by a strong twist (of a specific handedness) of the branches of its colonies [23, 30]. We refer to this property as strong chirality and name it the $\mathcal{C}$ morphotype. The most noticeable character of the other morphotype is its ability to form vortices; hence we refer to it as the $\mathcal{V}$ morphotype.

Each of the morphotypes exhibits its own profusion of patterns as the growth conditions are varied. These beautiful complex shapes reflect sophisticated strategies employed by the bacteria for cooperative self-organization as they cope with unfavourable growth conditions.

Lengthy and close inspection of the evolved patterns, combined with our understanding gained from the study of patterning in azoic systems and the use of the generic modelling approach, revealed to us novel biological features and provided explanations for the colonial pattern formation.

1.3. *Layout and rationale of the article*

Trying to convey the ideas in this article in a clear manner is no simple task, as they resulted from an interdisciplinary endeavour which, by its nature, does not fit 'linear presentation'. I chose to follow, in general, the course in which our studies have evolved. Doing so makes it easier for me to share with the reader the questions and wonderings which inspired our work. It is also useful for pointing out the existing open questions. While we have many promising results, the story is by no means complete. Part of my motivation for writing this article was to attract researchers to join this wonderful endeavour. I believe that indication of the intellectual challenges lying ahead can serve this goal.

From the beginning of the research we observed many beautiful patterns. The first effort was to turn these observations into a scientific program, the immediate target being to control the growth so that reproducible patterns can be obtained. It took over 2 years to develop a successful working protocol and to reach reproducibility [22, 23]. Once this was done, we could demonstrate (see section 2) velocity–pattern correlations, organization of the observations in a morphology diagram and the existence of morphology transitions. All these concepts are borrowed from the study of diffusive patterning in non-living systems described in part I [15].

Then comes the modelling of the growth, for which we combined our experimental observations (section 2), our general knowledge about bacterial movements and chemical-aided communication (briefly described in section 3) and the generic modelling approach. The first stage of the construction of the model is described in section 4. In section 5, I present the arguments in support of incorporating chemotactic signalling into the model and the resulting patterns. The arguments are based, to a large extent, on understanding gained from the study of patterning in non-living systems, demonstrating how the latter can help to reveal new biological features.

In section 6, I present studies of the colonial development of the C morphotype. The main messages are firstly that the $\mathcal{T} \rightleftharpoons C$ transitions involve a simple biological property, namely the length of the individual cells, and secondly the flagella handedness acts as a singular perturbation and leads to the observed chirality. The effect of chemotactic signalling on the C patterns is presented as a topic for future studies.

Section 7 is devoted to the studies of colonial development of the $\mathcal{V}$ morphotype. First I present our model of communicating gliders to describe collective migration observed in many kinds of gliding and swarming bacteria. Next, a few chemotactic mechanisms that we postulate for such bacteria are shown to lead to the formation of vortices.

Section 8 is comprised of conclusions and general discussion. I introduce the concepts of genome cybernetics, cybernators and their possible relations to the concept of complexity. Future research directions are discussed as well.

2. Patterns of the T morphotype

2.1. *Macroscopic observations*

Some examples of the patterns exhibited by colonies of the $\mathcal{T}$ morphotype are shown in figures 2–4. At very high peptone levels (above 10 g l^{-1}) the patterns are compact (figure 2 (*a*)). At somewhat lower but still high peptone levels (about 5–10 g l^{-1}) the patterns, reminiscent of Hele–Shaw patterns, exhibit quite pronounced radial symmetry and may be characterized as dense fingers (figure 2 (*b*)), each finger being much wider than the distance between fingers. For intermediate peptone levels, branching patterns with thin branches (reminiscent of electrochemical deposition) are observed (figure 2 (*c*)). The patterns are 'bushy', with branch width smaller than the distance between branches. As the peptone level is lowered, the patterns become more ramified and fractal like. Surprisingly, at even lower peptone levels (below 0.25 g l^{-1} for 2% agar concentration) the colonies revert to organized structures, fine branches forming a well defined global envelope. We characterize these patterns as fine radial branches (figure 2 (*d*)). For extremely low peptone levels (below 0.1 g l^{-1}), the colonies lose the fine radial structure and again exhibit fractal patterns (figure 3 (*a*)). For high agar concentration the branches are very thin (figure 3 (*b*)).

At high agar concentrations and very high peptone levels the colonies display a structure of concentric rings (figure 4 (*a*)). At high agar concentrations the branches exhibit a global twist with the same handedness, as shown in figure 4 (*b*)). Similar observations during growth of other bacterial strains have been reported by Matsuyama and co-workers [25, 26]. We referred to such growth patterns as having weak chirality, as opposed to the strong chirality exhibited by the C morphotype.

A closer look at an individual branch (figure 4 (*c*)) reveals a phenomenon of density variations within the branches. These three-dimensional structures arise from accumulation of cells in layers. The aggregates can form spots and ridges which are either scattered randomly, ordered in rows, or organized in a leaf-veins-like structure. The aggregates are not frozen; the cells in them are motile and the aggregates are dynamically maintained.

At the other extreme, of very soft agar (0.5% and below), the $\mathcal{T}$ morphotype does not exhibit branching patterns. Instead, the growth is compact with density variations as shown in figure 4 (*d*).

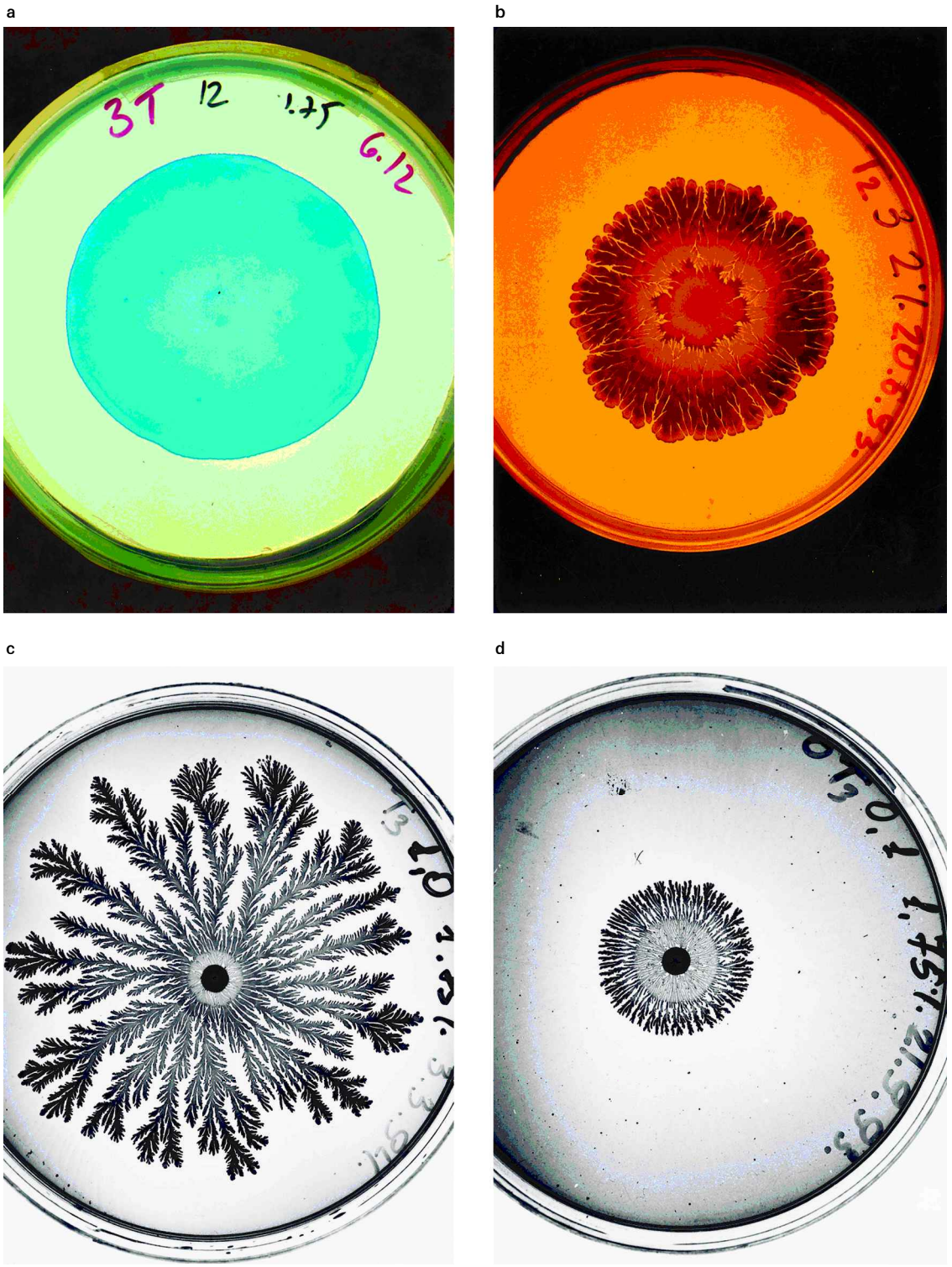

Figure 2. Examples of typical patterns of $\mathcal{T}$ morphotype for an intermediate agar concentration. (*a*) Compact growth for a peptone level of 12 g l^{-1} and an agar concentration of 1.75%. (*b*) Dense fingers for a peptone level of 3 g l^{-1} and an agar concentration of 2%. (*c*) Branching fractal pattern for a peptone level of 1 g l^{-1} and an agar concentration of 1.75%. (*d*) A pattern of fine radial branches for a peptone level of 0.1 g l^{-1} and an agar concentration of 1.75%.

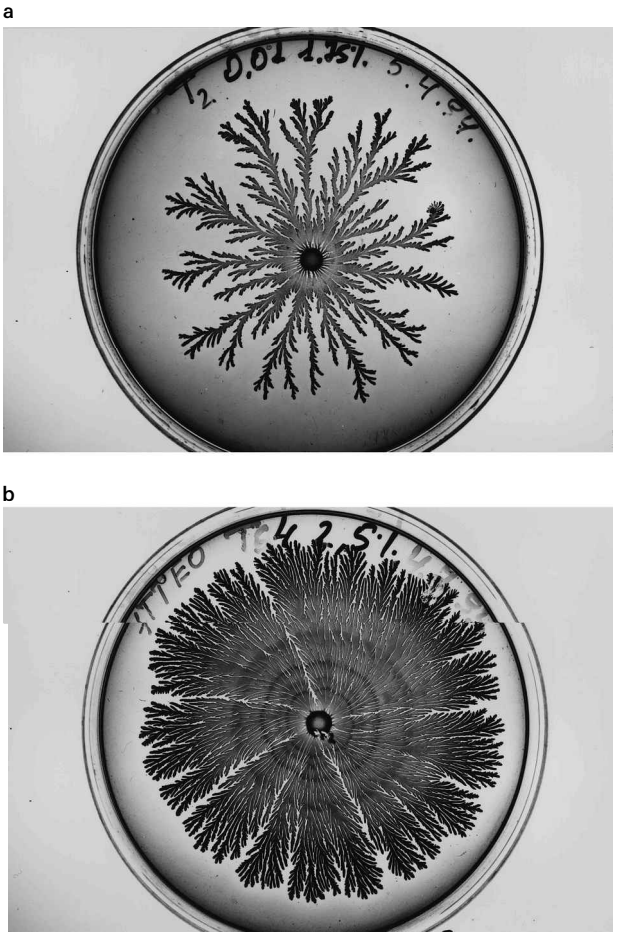

Figure 3. (*a*) Fractal pattern for a peptone level of 0.01 g l^{-1} and an agar concentration of 1.75%. (*b*) Dense branching pattern for a peptone level of 4 g l^{-1} and an agar concentration of 2.5%. Note that the branches are much thinner than those in figure 2(*b*), that is the branches are thinner for higher agar concentrations.

2.2. *Microscopic observations*

Under the microscope, cells are seen to perform a random-walk-like movement in a fluid. This fluid is, we assume, excreted by the cells and/or drawn by the cells from the agar [27, 28]. The cellular movement is confined to this fluid; isolated cells spotted on the agar surface do not move. The boundary of the fluid thus defines a local boundary for the branch. Whenever the cells are active, the boundary propagates slowly as a result of the cellular movement and production of additional wetting fluid.

The observations reveal also that the cells are active at the outer parts of the colony, while closer to the centre the cells are inactive and some of them sporulate (form spores). It is known that certain bacteria respond to adverse growth conditions by entering a spore stage until more favourable growth conditions return. Such spores are metabolically inert and exhibit a marked resistance to the lethal effects of heat, drying, freezing, deleterious chemicals and radiation.

2.3. *Morphology selection, morphology diagram and velocity–pattern correlations*

In part I [15], the emerging understanding of pattern determination in non-living systems was discussed at length, with special attention to the concepts of morphology diagram, morphology selection, morphology–velocity correlations and morphology transitions. In short, the patterns formed in many evolving azoic (non-living) systems may often be grouped into a small number of 'essential shapes' or morphologies, each representing a dominance of a different underlying effect. If each morphology is observed over a range of growth conditions, a morphology diagram may exist. The existence of a morphology diagram implies the existence of a morphology selection principle and vice versa. We proposed the existence of a new morphology selection principle: the principle of the fastest-growing morphology [14, 54]. In general, if more than one morphology is a possible solution, only the fastest-growing morphology is non-linearly stable and will be observed, that is selected.

The new selection principle implies that the average velocity is an appropriate response function for describing the growth processes and hence should be correlated with the geometrical character of the growth. In other words, for each regime (essential shape) in the morphology diagram, there is a characteristic functional dependence of the velocity on the growth parameters. At the boundaries between the regimes there is either discontinuity in the velocity (first-order-like transition) or in its slope (second-order-like transition).

At present, the above picture is widely accepted with respect to non-living systems (see part I). I believe that it is also valid for pattern determination during colonial development in bacteria. The bacterial patterns may be grouped into a small number of 'essential shapes', each observed over a range of growth conditions [18, 22, 23, 42, 55]. To prove my hypothesis, the next step would be to demonstrate the velocity–pattern correlation during colonial growth.

Ideally, the measurements of the growth velocity should be performed under constant-growth conditions. However, in practice, owing to humidity variations, finite size and edge effects, conditions do vary during growth [22, 23]. This introduces some uncertainty in the mapping of the morphology diagram. In the experiments presented in [23] we identified the morphology and measure its growth velocity when the colony fills about half the Petri dish.

We found that the velocity shows three distinct regimes of response, each corresponding also to a distinct morphology (the fine radial branches, branching patterns

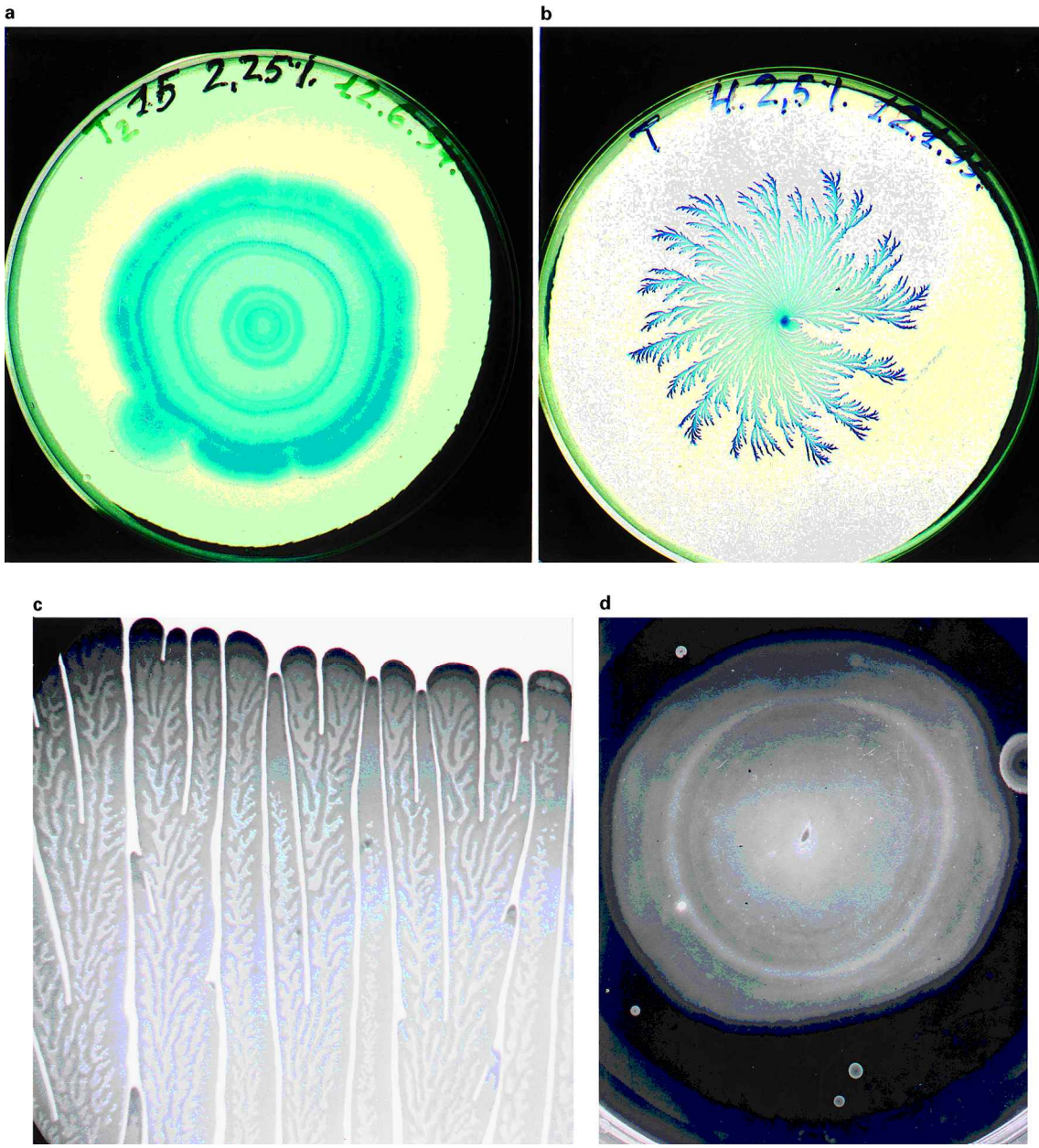

Figure 4. (*a*) **Concentric rings for a peptone level of 15 g l^{-1} and an agar concentration of 2.25%. (*b*) Weak chirality (global twist of the branches) for a peptone level of 4 g l^{-1} and an agar concentration of 2.5%. (*c*) Closer look at the branches (magnification of 50 ×) shows density variations within each branch. (*d*) Patterns produced during growth on soft agar (0.4%) and a peptone level of 5 g l^{-1}.**

and dense fingers), as was predicted for non-living systems. The change in velocity suggests that the switching between morphologies is indeed a real morphology transition and not a simple cross-over (see part I). The transition at low peptone level (between fine radial branches and branching structure) might be a first-order morphology transition, that is a transition characterized by a jump in the velocity and hysteresis. The transition at the higher peptone level (from branches to dense fingering) seems to be second order like. These observations of velocity–pattern correlations strongly support the existence of a morphology selection principle which determines the selected colonial morphology for a given morphotype.

In non-evolving (equilibrium) systems there is a phenomenon of critical fluctuations when the system is kept at the transition point between two phases. At that point the system consists of a mixture of the two phases. In part I it was shown that an analogous phenomenon exists in

evolving non-living systems (see also figure 5) and explained that this fact provides additional support for the idea of morphology transitions. Figure 5 shows patterns exhibited by colonies grown at 'critical' peptone levels, where transitions between two morphologies occur. Similarly, for the fluctuations displayed by non-living systems, we observe a combination of the morphologies characterizing the patterns above and below the critical point. These observations provide additional support for the relevance of the concepts of morphology selection and morphology transition to colonial development. In section 5, I shall demonstrate that chemotactic interplay is the biological origin of the observed morphology transitions. Before doing so, I shall briefly describe bacterial movements and chemotactic response in the next section and introduce the communicating walkers' model in section 4.

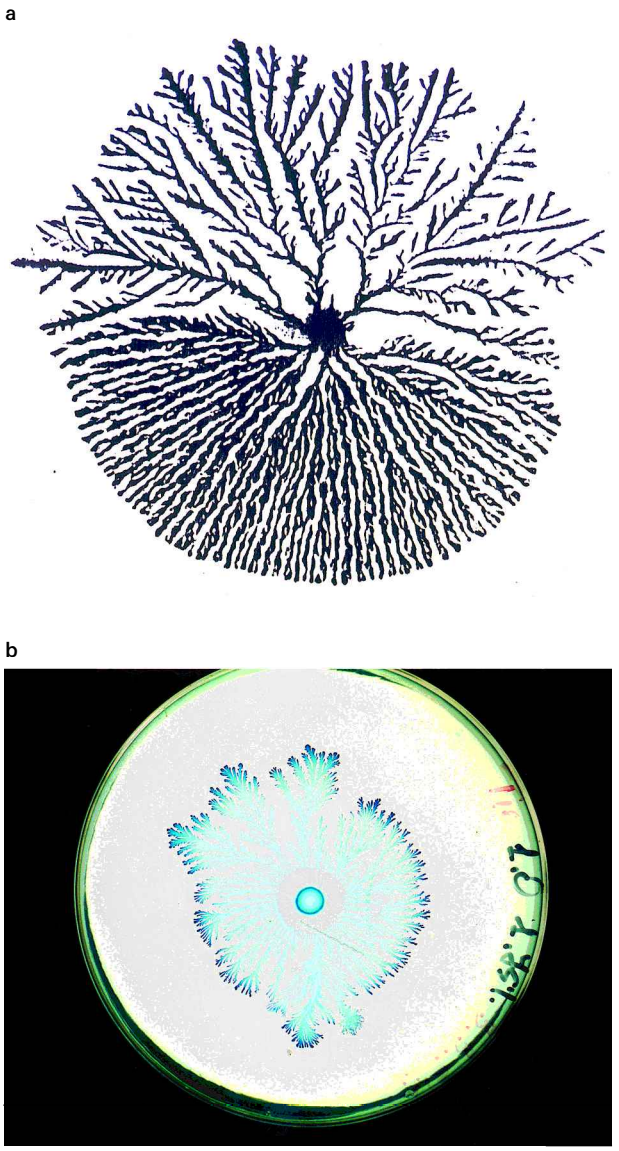

Figure 5. (*a*) Electrochemical deposition growth of zinc sulphate for 15 V and 0.1 mol. This value of the voltage corresponds to the boundary between dense branching and dendritic growth. The observed pattern is made up of a combination of the two morphologies. This phenomenon is the analogue of critical fluctuations at second-order phase transitions (see part I). (*b*) A pattern combined of branching pattern and a pattern of fine radial branches, developed during growth of colonies at a peptone level of 1 g l^{-1} and an agar concentration of 1.75%. This level of peptone is on the boundary between the two corresponding morphologies.

3. Bacterial movement and chemotaxis

3.1. *Classification of bacterial movements*

In the course of evolution, bacteria have developed ingenious ways of moving on surfaces. The most widely studied and perhaps the most sophisticated translocation mechanism used by bacteria is the flagella [56], but other mechanisms exist as well [57]. I describe here briefly the different types of bacterial surface translocation, which classically are defined as follows [57].

(1) *Swimming*. Surface translocation is produced through the action of flagella. The cells move individually and at random in the same manner as flagellated bacteria move in wet mounts (i.e. nearly straight runs separated by brief tumbling). Swimming takes place only in sufficiently thick surface fluid. Microscope observations reveal no organized flow-field pattern.

(2) *Swarming*. Surface translocation is produced through the action of flagella but, unlike swimming, the movement is continuous and regularly follows the long axis of the cell. The cells are predominantly aggregated in bundles during their movement, and microscope observations reveal flow-field patterns highly organized in whirls and bands.

(3) *Gliding*. Surface translocation occur only in non-flagellated bacteria and only when in contact with solid surface. In all other respects, gliding is identical with swarming.

(4) *Twitching*. Surface translocation occur in both flagellated and non-flagellated bacteria, but not through the action of flagella. The movement is usually solitary (although small aggregates may occur), appears intermittent and jerky and does not regularly follow the long axis of the cell.

(5) *Sliding*. Surface translocation is produced by the expansive forces in a growing culture in combination with special surface properties of the cells that reduce the friction between cell and substrate. The microscopic observations reveal a uniform sheet of closely packed cells in a single layer that moves slowly as a unit.

(6) *Darting*. Surface translocation is produced by the

expansive forces developed in an aggregate of cells inside a common capsule. These forces cause ejection of cells from the aggregate. The resulting pattern is that of cells and aggregates of cells distributed at random with empty areas of substrate in between. Neither cell pairs nor aggregates move expect during the ejection which is observed as flickering in the microscope.

These types of bacterial movement can be organized in two major categories: solitary or clustered. In the case of solitary movement, no long-range correlations exist between the movement of different cells, and the resulting density can be approximated by a simple diffusion equation. In contrast, in the case of clustered movement the interactions between cells have a profound influence on the movement and the resulting dynamics; thus the equations describing the cellular density are not nearly as simple.

As for the movement of the $\mathcal{T}$ morphotype, on the basis of microscopy and electron microscopy observations of flagella we identify the movement as swimming. The cellular velocity is very sensitive to the growth conditions and to the location in the colony; typically, it is of the order of $1-10\ \mu m\ s^{-1}$. Cells tumble about every $\tau_T \approx 1-5$ s, which translates to an effective diffusion constant D_B of the order of $10^{-8}-10^{-5}\ cm^2\ s^{-1}$. This is correct for low densities such that the average distance between cells, or collision length ($l_c \equiv \rho^{-\frac{1}{3}}$ in three dimensions and $l_c \equiv \sigma^{-\frac{1}{2}}$ in two dimensions) is longer than the tumbling length. In this case the cellular concentration diffusion coefficient is

$$D_B \propto v^2 \tau_T \equiv D_T \tag{1}$$

where v is the cellular velocity between tumbling events (the duration of which is considered negligible). In the opposite limit, $l_c < l_T = \mathcal{V}\mathcal{T}_T$, the time of straight motion is l_c/v instead of τ_T. Hence D_B depends on the cellular concentration of yield.

$$\begin{aligned} D_B &\propto v\rho^{\frac{1}{3}} \text{ in three dimensions,} \\ D_B &\propto v\sigma^{\frac{1}{2}} \text{ in two dimensions.} \end{aligned} \tag{2}$$

Here we assumed that v is constant. However, it can depend on the cellular density via the amount and quality of extracellular slime emitted by the cells. In such cases the above expressions should be modified accordingly.

3.2. *Chemical-aided communication, regulation and control*

Many means of chemical communication are employed by bacteria (see [58] and references therein). Here we mention only a few examples. *B. subtilis* and *Myxococcus xanthus*, like many other species of bacteria, sporulate (see definition in section 2.2.) as a way to survive conditions that they cannot live through. They do not do it as solitary cells. *B. subtilis* sporulate in response to extracellular differentiation factors, two signals that are sent by other cells and relay information about the cellular density and the state of the colony [59]. *M. xanthus* uses several similar signals during the sporulation process. The A signal, for example, is used at early stages to estimate the density of the surrounding cells, and the sporulation process is not activated until critical density is achieved [58, 60]. *Escherichia coli*, when exposed to oxidative stress, emit the amino acid aspartic acid that attract neighbouring cells and allow the cooperative degradation of toxic materials [39].

In all the above examples and in many others, the colony creates fields of chemicals that provide the bacterial cells with global information, that is information about an area much larger than the cell size, which could not have been gathered directly by a single cell.

Another very important chemical response is chemotactic signalling. Chemotaxis means changes in the movement of the cell in response to a gradient of certain chemical fields [61–64]. The movement is biased along the gradient either in the gradient direction or in the opposite direction. Usually chemotactic response means a response to an externally produced field as in the case of food chemotaxis. However, it could also be a response to a field produced directly or indirectly by the bacterial cells. We shall refer to the latter as chemotactic signalling.

3.3. *Perception of chemical concentration and its gradient*

A bacterial cell senses the local concentration C of a chemical via membrane receptors binding the chemical's molecules. Typically, the receptors are specific, but some receptors can bind more than one chemical. The cell 'senses' the concentration by measuring the fraction of occupied receptors $N_o/(N_o + N_f)$, where N_o and N_f are the number of occupied and free receptors respectively. For a given C, N_o is determined by two characteristic times: the average time τ_o of occupation and the average time τ_f when the receptor is free. Since τ_f is inversely proportional to the concentration of the chemical (with the proportion coefficient determined by the receptor affinity to the chemical), we get

$$\frac{N_o}{N_f + N_o} = \frac{\tau_o}{\tau_f + \tau_o} = \frac{C}{K + C}, \tag{3}$$

where $K \equiv C\tau_f/\tau_o$.

The bacterial cells are too short simply to compare the concentration at different locations on their membrane. According to the contemporary wisdom they perform successive temporal measurements along their path. *E. coli*, for example, are known to be capable of successive measurements and their comparison over a time interval of 3 s can be performed. For attractive chemotaxis, the larger the detected increase in concentration between two measurements, the longer the tumbling is postponed. In

other words, chemotaxis is implemented by decreasing the tumbling frequency as cells swim up the gradient of the attractant.

In the model presented below, we implement the chemotactic response by changing the directional probability of the walkers' displacement; there is a higher probability of performing a step towards higher concentrations of the chemoattractant. We use this implementation in order to simplify the numerical scheme, but it is equivalent to the bacterial implementation over moderate times or concentrations.

It is crucial to notice that the cells actually measures changes in $N_o/(N_o+ N_f)$ and not in the concentration itself. Using equation (3) and assuming that τ_o does not change in space, we obtain

$$\frac{\partial}{\partial x}\left(\frac{N_o}{N_o + N_f}\right) = \frac{K}{(K + C)^2}\frac{\partial C}{\partial x}. \qquad (4)$$

This means that the chemical gradient times a prefactor $K/(K+ C)^2$ is measured. This is known as the 'receptor law' [65]. For very high concentrations the chemotactic response vanishes owing to saturation of the receptors. The chemotactic response must also vanish at the opposite limit of small concentration, as the concentration reception is masked by external and internal noises.

3.4. *Chemotaxis towards nutrient*

Chemotaxis towards a high concentration of nutrients is a well studied phenomenon in bacteria [61, 66]. When the centre of a semisolid agar plate (0.35% agar concentration) is inoculated with chemotactic cells, distinct circular bands of bacterial cells become visible after incubation for a few hours. In fact, these patterns were used as semiquantitative indicators of chemotactic response [66]. Genetic experiments showed that the creation of each of those bands depends solely on the chemotactic response to a single chemical in the substrate (these chemicals are usually metabolizable, but even cells that have lost the ability to metabolize a certain chemical form bands, as long as they are attracted to it [61]. The order of the bands and the apparent distance between the bands is determined by the cells' preferences to different nutrients. It can be easily shown that linear chemotactic response to a nutrient cannot produce such bands. A nonlinear response such as the 'receptor law' must be included for the bands to form. Moreover, a high concentration of the attractant represses both the strength of the chemotactic response [61] and the velocity of the expanding band [67]. These observations are accounted for by the 'receptor law' for chemotactic response if one assumes that the average gradient sensed by the cells is proportional to the initial concentration of the chemical [61, 67].

4. The communicating walkers' model

4.1. *Computer games versus generic modelling*

With present computational power it is natural to use computer models as a main tool in the study of complex systems. How should one approach modelling of the complex bacterial patterning? First, one must be careful not to fall in the trap of the 'reminiscence syndrome', described by J. Horgan [68] as the tendency to devise a set of rules which will mimic some aspects of the observed phenomena and then, to quote Horgan, 'They say: ''Look, isn't this reminiscent of a biological or physical phenomenon!'' They jump in right away as if it's a decent model for the phenomenon, and usually of course it's just got some accidental features that make it look like something'. Still, the reminiscence modelling approach has some indirect value. Even if it does not reveal directly the biological functions and behaviour, it does reflect understanding of geometrical and temporal features of the patterns, which indirectly might help in revealing the underlying biological principles.

Another extreme to avoid is the 'realistic modelling' approach, where one constructs an algorithm that includes in detail all the known biological facts about the system. A model like this will keep evolving to include more and more details until it loses all predictive power.

Here we try to promote another approach: 'generic modelling' [9, 27, 69]. We seek to elicit, from experimental observations and biological knowledge, the generic features and basic principles needed to explain the biological behaviour, and we included these features in the model. We shall show that such modelling together with close comparison with experimental observations, can be used as a research tool to reach new understanding of the biological systems.

Generic modelling is not about using sophisticated, as it may, mathematical descriptions to dress pre-existing understandings of complex biological behaviour. Rather, it means using existing biological knowledge together with mathematical tools and synergistic point of view to reach new understanding (reflected in the constructed model) of observed complex phenomena.

4.2. *The walkers, the boundary and local interaction*

The communicating walkers' model was inspired by the diffusion–transition scheme used to study solidification from supersaturated solutions [70–72]. The former is a hybridization of the 'continuous' and 'atomistic' approaches used in the study of non-living systems. The diffusion of the chemicals is handled by solving a continuous diffusion equation (including sources and sinks) on a triangular lattice of a lattice constant a_0. The bacterial cells are represented by walkers, allowing a more detailed

description. In a typical experiment, at the end of the growth in a Petri dish there are $10^9 - 10^{10}$ cells, a number impractical to incorporate into the model. Instead, each of the walkers represents about $10^4 - 10^5$ cells, so that we work with $10^4 - 10^6$ walkers in one numerical 'experiment'.

The walkers perform an off-lattice random walk within a boundary representing that of the lubrication fluid. This boundary is defined on the same tridiagonal lattice where the diffusion equations are solved. To incorporate the swimming of the cells into the model, at each time step each of the active walkers (motile and metabolizing) moves from its location $\mathbf{r}_i$ a step of size $d < a_0$ at a random angle θ to a new location $\mathbf{r}'_i$ is given by

$$\mathbf{r}'_i = \mathbf{r}_i + d(\cos\theta; \sin\theta). \tag{5}$$

If the new location $\mathbf{r}'_i$ is outside the boundary, the walker does not perform that step, and a counter on the segment of the boundary which would have been crossed by the movement $\mathbf{r}_i \rightarrow \mathbf{r}'_i$ is increased by one. When the segment counter reaches a specified number of hits N_c, the boundary propagates one lattice step and an additional lattice cell is added to the area occupied by the colony. This requirement of N_c hits represents the colony propagation through wetting of unoccupied areas by the cells. Note that N_c is related to the agar concentration as more lubrication fluid has to be produced (more 'collisions' are needed) to push the boundary on a harder substrate.

4.3. *Food consumption, internal energy, reproduction and sporulation*

We represent the metabolic state of the ith walker by an 'internal energy' E_i. The rate of change of this energy is given by

$$\frac{\mathrm{d}E_i}{\mathrm{d}t} = \kappa C_{\text{consumed}} - \frac{E_m}{\tau_R}, \tag{6}$$

where κ is a conversion factor from food to internal energy ($\kappa \approx 20 \times 10^3$ J g^{-1}) and E_m (about 60 nJ) represents the total energy loss for all processes (excluding reproduction) over the minimal time of reproduction τ_R (about 20 min). The food consumption rate C_{consumed} is

$$C_{\text{consumed}} \equiv (\Omega_C, \Omega'_C). \tag{7}$$

Ω_C is the maximum rate of food consumption which is about $10^{-11} - 10^{-10}$ g s^{-1}, and Ω'_c is the maximal rate of food consumption as limited by the locally available food. The estimate of Ω_C was the crucial step in relating the model's parameters with real bacterial growth. The mass of a bacterial cell is about 10^{-12} g (1 pg). We assume that each cell consumes about 3 pg of food for reproduction: 1 pg for the mass of the new cell, 1 pg for metabolism and 1 pg to 'pay' for decreasing the entropy while transforming food into a cell. The maximal consumption rate per one cell is 3 pg during the minimal reproduction time τ_R, which is about 20 min. Ω_C is the maximal consumption rate per cell times the number of cells represented by a single walker.

When sufficient food is available, E_i increases until it reaches a threshold energy, at which time the walker divides into two. When a walker is starved for a long interval of time, E_i drops to zero and the walker 'freezes'. This 'freezing' represents the sporulation process. For simplicity (and on the basis of experimental observations), we assumed that in our experiments the cellular density is suitable for sporulation, so that the limiting factor is the supply of nutrients.

Although the food source in the experiments is peptone (and not a single carbon source), we represent the diffusion of nutrients by solving the diffusion equation for a single agent whose concentration is denoted $C(\mathbf{r}, t)$:

$$\frac{\partial C}{\partial t} = D_C \nabla^2 C - \sigma_a C_{\text{consumed}}, \tag{8}$$

where the last term includes the consumption of food by the active walkers whose density is denoted σ_a. The equation is solved on the triangular lattice using zero-flux boundary conditions. The simulations are started with a uniform distribution C_0, denoted in the figures by P, for peptone. $P = 10$ corresponds approximately to 1 g l^{-1}. In the Petri dish [23] we pour about 22 ml of the agar mixture. Hence 1 g l^{-1} can support growth of about 10^9 bacterial cells. In a typical run we use a lattice of size 500×500. Thus $P = 10$ corresponds to about 10^{-7} g per lattice cell or about one walker per lattice cell. During the numerical growth there are about ten walkers per lattice cell, which means that indeed for the 1 g l^{-1} peptone level the growth is diffusion limited. The diffusion constant D_C is typically (depending on agar dryness) $10^{-4} - 10^{-6}$ cm^2 s^{-1}, which is comparable with the bacterial effective diffusion constant (section 3).

4.4. *Results of numerical simulations*

Results of numerical simulations of the model are shown in figure 6. One time step in the simulations is the bacterial tumbling tie τ_T (section 3) which corresponds to about 1 s. A typical run is up to about $10^4 - 10^6$ time steps which translates to about 2 days of bacterial growth. Such simulations on a work station take about 2.5 h, which is 20 times faster than 'real life'. To complete the correspondence between the model's parameters and real growth we should estimate N_c. The lattice constant a_0 is about ten times (about 100 μm) the walker's tumbling step. Hence for ten walkers in one lattice cell we have about 0.25 – 2 collisions on each segment of the envelope. From time-lapse measurements of the growth, the envelope propagates at a rate of 2 – 20 μm min^{-1} for 1.5% agar. Thus the corresponding N_c is about 20.

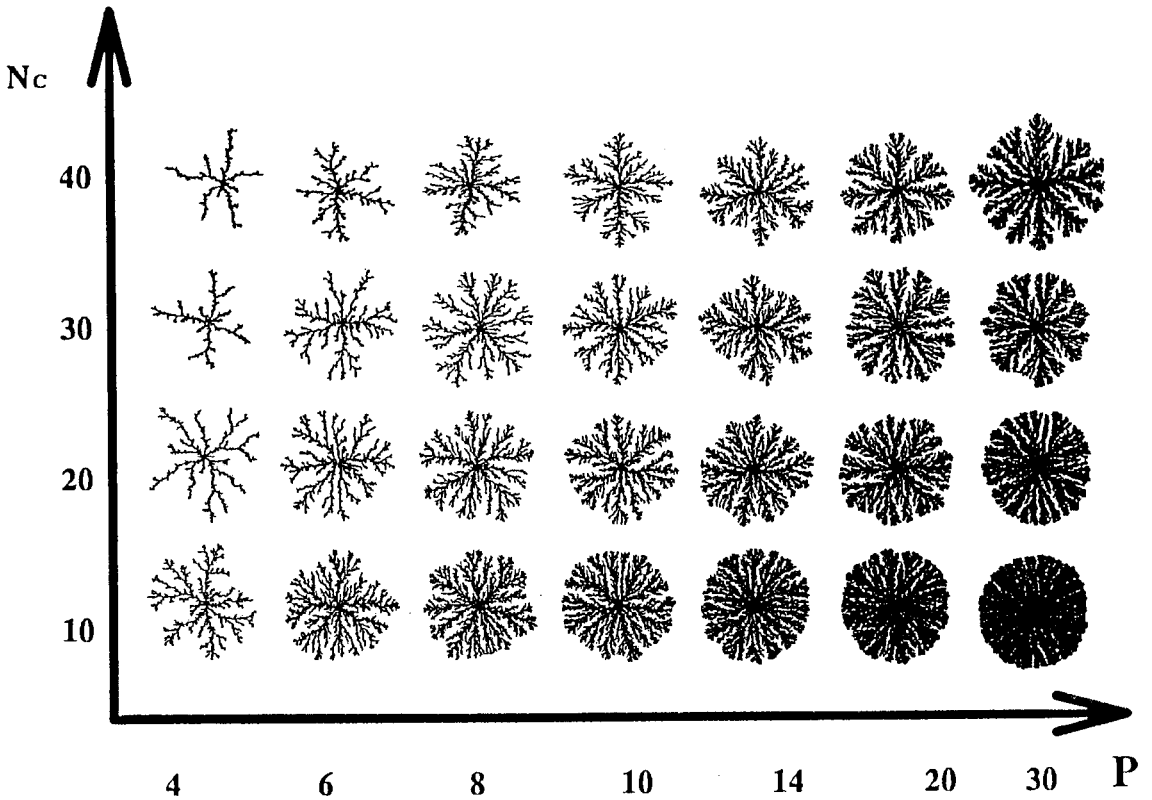

Figure 6. Results of numerical simulations of the communicating walkers' model. P is the peptone level. P = 10 corresponds to about 1 g l^{-1}. N_c is related to the agar concentration. N_c = 15 corresponds to an agar concentration of about 1.5%.

As in real bacterial colonies, the patterns are compact at high peptone levels and become fractal with decreasing food level. For a given peptone level, the branches are thinner as the agar concentration increases. Clearly, the results shown in figure 6 are very encouraging and do capture some features of the experimentally observed patterns. The branching patterns and the constant growth velocity are a manifestation of the diffusion field instability which we have mentioned in the introduction (see also part I). However, some critical features, such as the ability of the bacteria to develop organized patterns at very low peptone levels (instead of more ramified structures as would be suggested by the diffusion instability), the changes in the functional form of the growth velocity as a function of nutrient concentration and the three-dimensional structures are not accounted for by the model at this stage. We propose that chemotactic response should be included in the model in order to explain these additional features.

5. Chemotaxis-based adapative self-organization

We assumed that for the colonial adaptive self-organization the $\mathcal{T}$ morphotype employs three kinds of chemotactic response. One is the food chemotaxis that I have mentioned earlier. According to the 'receptor law' (section 3), it is expected to be dominant for the intermediate range of nutrient levels (the corresponding levels of peptone are determined by the constant K). The two other kinds are self-induced chemotaxis or signalling chemotaxis, that is chemotaxis towards agents produced by the bacterial cells themselves. As I shall show, for efficient self-organization it is useful to have two chemotactic responses operating on different length scales, one regulating the dynamics within the branches (short length scale) and the other regulating the organization of the branches (long length scale). The length scale is determined by the diffusion constant of the chemical agent and the rate of its spontaneous decomposition (the decay time of a chemical is an important factor in its usefulness as information conveyer, and thus in its usefulness as a self-organization aid for the bacterial colony). If there is also decomposition of the chemical by the cells, it gives them additional control of the length scale. In section 3, I have mentioned both attractive and repulsive chemotatic response. We have reasons to expect that both kinds will be employed by the bacteria; so we proceed to find the correspondence between the short range against long range and attractive against repulsive. To do so we return to the experimental observations.

5.1. *Attractive chemotactic signalling*

The length scale of the three-dimensional structures indicates the existence of a dynamical process with a characteristic length shorter than the branch width. The accumulation of cells in the aggregates brings to mind the existence of a short-range self-attracting mechanism. In addition, observations of attractive chemotactic signalling in *E. coli* [29, 39–41, 73] indicate that it operates during growth at high levels of nutrients. Under such conditions the bacterial cells produce hazardous metabolic waste products. The purpose of the attractive signalling is to gather cells to help in the decomposition of the waste products. This scenario is consistent with the observation of three-dimensional structures during growth at high peptone levels. Motivated by the above, we assume that the colony employs an attractive self-generated short-range chemotaxis during growth at high levels of nutrients. To test this hypothesis we add the new feature to the communicating walkers' model and compare the resulting patterns with the observed patterns.

Following [29, 73], we include the equation describing the time evolution of the concentration $A(\mathbf{r},t)$ of the attractant:

$$\frac{\partial A}{\partial t} = D_{\mathrm{A}}\,\nabla^2 A + \sigma_{\mathrm{T}}\Gamma_{\mathrm{A}} - \sigma_{\mathrm{a}}\Omega_{\mathrm{A}} A - \lambda_{\mathrm{A}} A, \qquad (9)$$

where σ_{a} is the density of the active walkers and σ_{T} is the density of the walkers triggered to emit the attractant. Γ_{A} is the emission rate of attractant by triggered walkers, Ω_{A} is the decomposition rate of attractant by all the active bacteria and λ_{A} is the rate of spontaneous decomposition of attractant. The walkers are triggered either when the level of attractant is above a threshold (autocatalytic response) or when the level of a triggering field is above a threshold (see [29, 73] for details). The triggering field W, which represents the concentration of waste products, satisfies the following equation:

$$\frac{\partial W}{\partial t} = D_{\mathrm{W}}\,\nabla^2 W + \Gamma_{\mathrm{W}}\sigma_{\mathrm{a}} C_{\mathrm{consumed}} - \sigma_{\mathrm{a}}\Omega_{\mathrm{W}} W - \lambda_{\mathrm{W}} W. \qquad (10)$$

Γ_{W}, Ω_{W} and λ_{W} have meanings corresponding to Γ_{A}, Ω_{A} and λ_{A}, respectively.

As was mentioned in section 3, in the presence of the attractant the movement of the active walkers changes from pure random walk (equal probability to move in any direction) to a random walk with a bias along the gradient of the communication field (higher probability to move towards higher concentrations of the attractant). In figure 7 we show an example of the formation of three-dimensional structures when the attractive chemoresponse is included in the model.

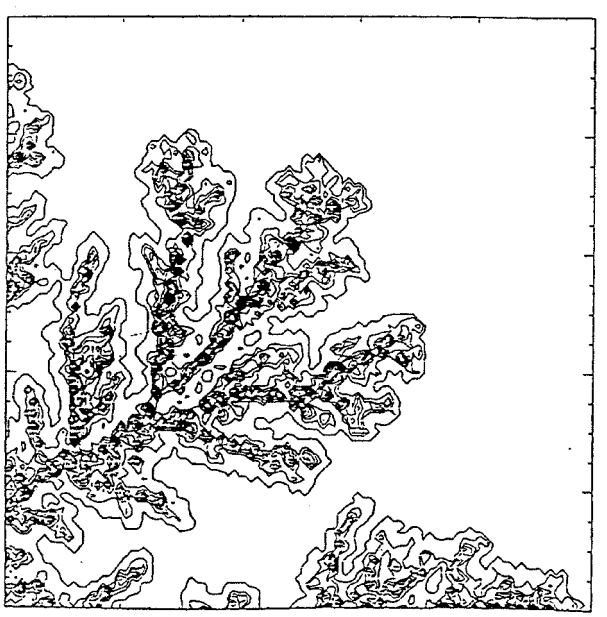

Figure 7. The effect of attractive chemotaxis in the model. The figure shows curves of equal bacterial density to demonstrate the formation of three-dimensional patterns. The size is 120 ×120 lattice units.

5.2. *Repulsive chemotactic signalling*

We focus now on the formation of the fine radial branching patterns at low peptone levels. From the study of non-living systems it is known that, in the same manner that an external diffusion field leads to the diffusion instability, an internal diffusion field will stabilize the growth. It is natural to assume that such a field is produced by some sort of chemotactic agent. To regulate the organization of the branches, it must be long range. We assumed that the chemoattractive response is short range, which implies that the new response is repulsive and long range. Moreover, I mentioned that sporulation is a drastic and cooperative phenomenon reserved for extreme stress conditions. When the stress is food depletion, it is biologically reasonable that, before going through sporulation, cells emit (either purposely or as a byproduct) a material which causes other cells to move away; so they can have the remaining food for themselves. To test this idea, a chemorepellent response has been included in the model [27].

The equation describing the time evolution of the concentration field $R(\mathbf{r},t)$ of the chemorepellent is

$$\frac{\partial R}{\partial t} = D_{\mathrm{R}}\,\nabla^2 R + \sigma_{\mathrm{s}}\Gamma_{\mathrm{R}} - \sigma_{\mathrm{a}}\Omega_{\mathrm{R}} R - \lambda_{\mathrm{R}} R, \qquad (11)$$

where σ_{s} is the density of the stationary cells, Γ_{R} is the emission rate of the chemorepellent and Ω_{R} is the decomposition rate of the chemorepellent by the active walkers. The last term represents spontaneous decomposition of the chemorepellent at a rate λ_{R}.

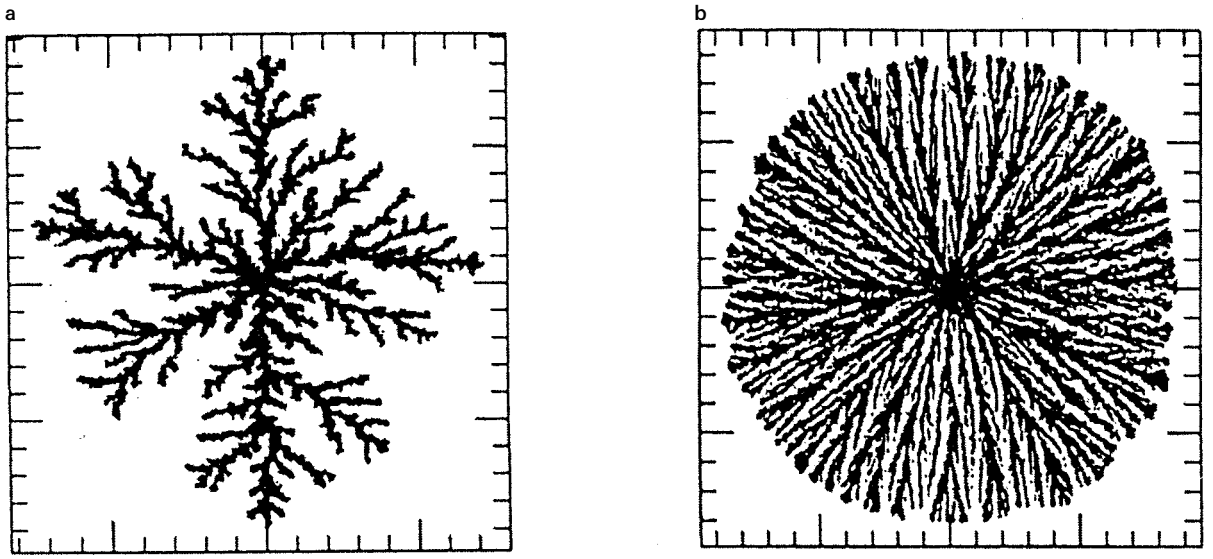

Figure 8. The effect of repulsive chemotaxis in the model for $P = 10$ and $N_c = 40$. (*a*) Without chemotaxis. (*b*) When repulsive chemotaxis is included. The size is 400 ×400 lattice units.

In the presence of the chemorepellent, the movement of the active cells changes from a pure random walk to a random walk with a bias to move away from a high concentration of chemorepellent.

In figure 8 we demonstrate the dramatic effect of the repulsive chemotactic signalling. The pattern becomes much denser with a smooth circular envelope, while the branches are thinner and radially oriented. This structure enables the colony to spread over the same distance with fewer walkers. Thus the emission of chemorepellent by the stressed walkers also serves the interest of the colony as it can cope better with the growth conditions.

The patterns produced by the simulations seem to be in agreement with the experimental observations. Yet the numerical simulation poses a difficulty; as can be expected the radially outwards 'push' of the walkers by the repulsive signalling leads to a faster spread of the colony. This result does not agree with the experimental observations; the velocity of the fine radial branching patterns is lower than that of the fractal growth observed at higher peptone levels. Moreover, in figure 4 we show a colony with sectors of fractal growth embedded in a fine radial branching structure. Clearly, the fractal growth is faster. This dilemma is resolved when food chemotaxis is included as well.

5.3. *Amplification of diffuse instability due to nutrients chemotaxis*

In non-living systems (e.g. the diffusion-limited aggregation of many walkers, electrochemical deposition or the Hele–Shaw cell), typically, the more ramified the pattern (with a lower fractal dimension), the lower is the growth velocity. Now we are looking for a mechanism which is capable of doing just the opposite, namely a mechanism which can both increase the growth velocity and maintain, or even decrease, the fractal dimension. We expected food chemotaxis to be the required mechanism. It provides an outward drift to the cellular movements; thus it should increase the rate of envelope propagation. At the same time, being a response to an external field it should also amplify the basic diffusion instability of the nutrients field. Hence, it can support faster growth velocity together with a ramified pattern of low fractal dimension.

Again, we used the communicating walkers' model as a research tool to test the above hypothesis. As expected, the inclusion of food chemotaxis led to a considerable increase in the growth velocity without significant change in the fractal dimension of the pattern (figure 9).

5.4. *Chemotactic interplay, wetting fluid and morphology transitions*

As mentioned earlier, we expect food chemotaxis to dominate the growth for intermediate peptone levels. According to the 'receptor law', its effect should decrease at higher levels of peptone. In this limit we expect the self-generated attractive chemotaxis to become the dominant mechanism. The morphology transition between the fractal branched growth and the radial fingers growth presumably result from switching the leading role between the two

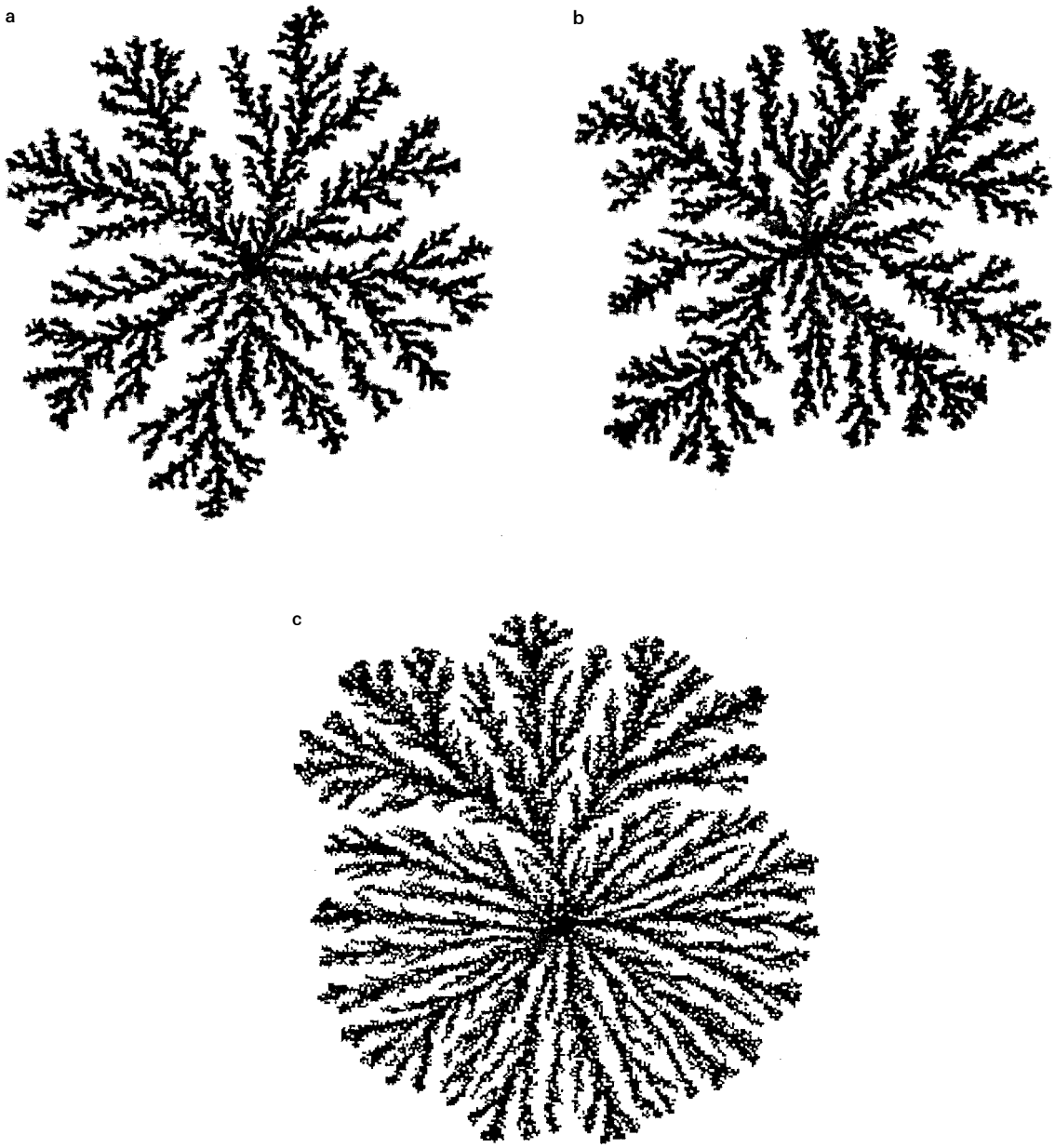

Figure 9. The effect of food chemotaxis in the model. (*a*), (*b*) For $P = 10$ and $N_c = 40$. In (*b*) food chemotaxis is included. The growth is twice as fast as that of (*a*), and yet the patterns have the same fractal dimension. (*b*) The pattern after half the growth time of (*a*). (*c*) The faster sector consists of walkers for which the food chemotaxis mechanism is turned on while for the rest of the colony there is only repulsive chemotaxis. Note the similarity with the observed pattern shown in figure 5.

kinds of chemotaxis response. The fact that we observe a real transition and not a cross-over means that there is another mechanism which regulates the interplay between the two responses. The observations of increased branch width upon transition indicate that regulation of the emission of the wetting fluid might also be part of the transition.

The morphology transition from the fine radial branching growth to the fractal branching growth is probably related to a switching from dominance of repulsive signalling chemotaxis to that of food chemotaxis. Again, the sharpness of the transition indicates that an additional regulating mechanism might be involved.

In figure 10, various morphologies are displayed, each

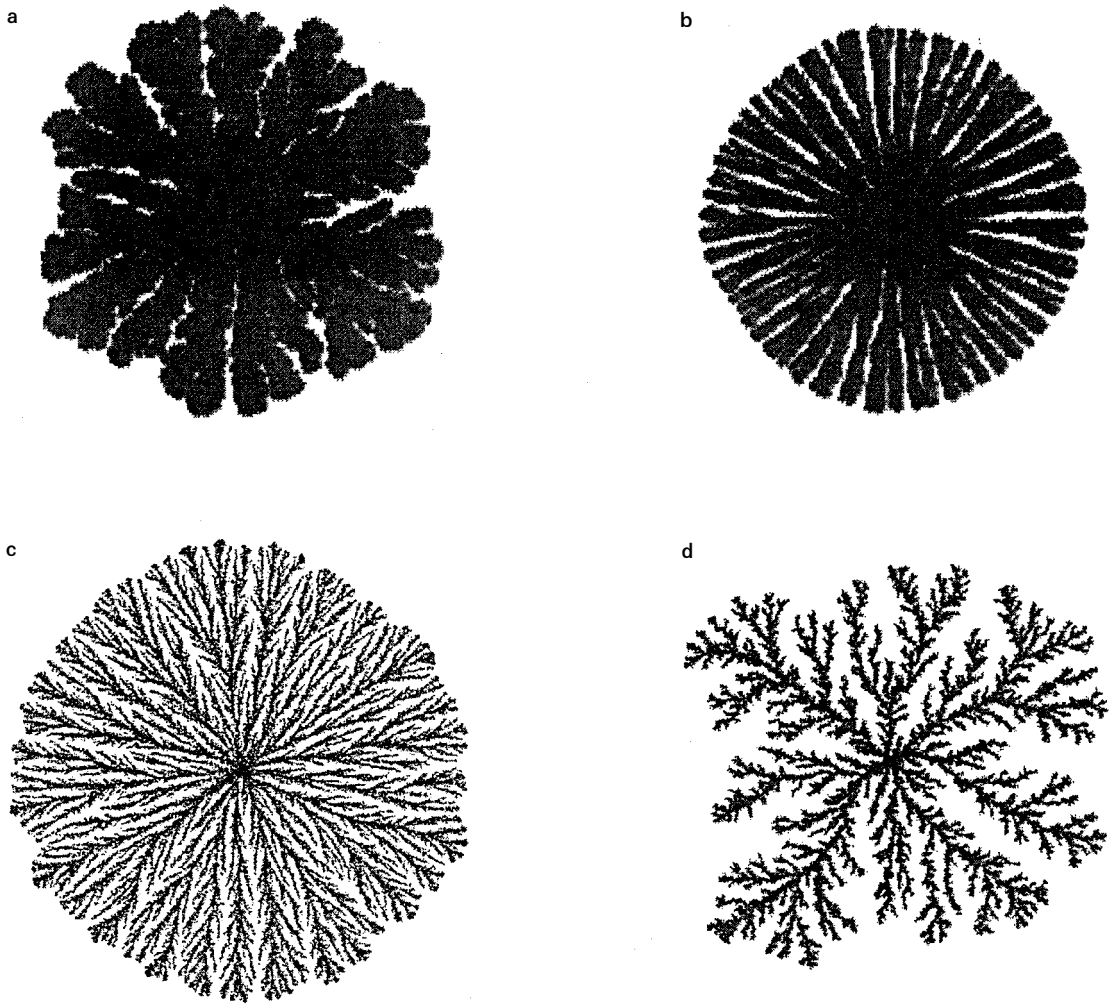

Figure 10. Example of patterns produced by the model for various combinations of repulsive chemotaxis and food chemotaxis. In (*a*), (*b*) the system sizes are half the system sizes of (*c*), (*d*), which are reduced to appear in uniform size. In (*a*), repulsive signalling chemotaxis is turned on; in (*b*), food chemotaxis is turned on (although quite weak); in (*c*), both are turned on.

for a different combination of chemotactic responses. In doing so we capture most of the observed patterns, yet the additional mechanisms regulating the relative strengths of the responses, and the emission of the wetting fluid still have to be explored.

5.5. *Bacterial 'snowflakes'*

Motivated by the studies of diffusive patterns in non-living systems, we set out to test the predictions of the communicating walkers' model regarding growth in the presence of anisotropy [74]. An essential part of the new understanding of diffusive patterning in non-living systems involves the role of anisotropy [12–15]. Anisotropy is responsible for the appearance of dendritic growth rather than a cascade of tip splitting.

Motivated by the above, we studied the effect of two types of anisotropy using the communicating walkers' model: firstly a sixfold line anisotropy, in which N_c is smaller along three intersecting narrow strips (the diagonals of an hexagonal), and secondly a fourfold lattice anisotropy, in which N_c is smaller along two sets of parallel narrow strips. The sets are perpendicular to each other and form a fourfold lattice. In both cases we study theoretically the effect of repulsive chemotaxis. For the sixfold line anisotropy we show that the effect of the anisotropy fades away at low peptone levels unless chemorepulsion is included in the model (figure 11). In the case of fourfold lattice anisotropy we show a concave-to-convex transition (as a function of peptone level) when repulsive chemotaxis is included in the model (figure 12).

To test the above predictions we looked for a method

to impose controlled weak broken symmetry on the agar surface. Previously [22] we observed dendritic growth in response to uncontrolled (spontaneous) anisotropy which is formed as the agar is drying. Now we looked for controlled anisotropy, one that can also be mimicked by the model's simulations. After experimenting with various approaches, we developed an efficient method of 'agar stamping' [74]. This effect (which is the analogue of anisotropy in surface tension) is captured by the model via the variations in N_c.

In figure 13 we show typical growth patterns observed during growth in the presence of imposed sixfold anisotropy. Although the patterns resemble real snowflakes, I emphasize that the imposed anisotropy differs from the inherent crystalline anisotropy of the ice crystals. At high peptone levels, the patterns are denser and the effect of the anisotropy fades away. At very low peptone levels, the patterns become denser again and maintain the sixfold symmetry, in agreement with the simulations when repulsive chemotaxis is included.

Next, we present observations of growth in the presence of fourfold lattice anisotropy. Following the theoretical predictions, we studied the growth as a function of peptone level (figure 14). A clear concave-to-convex transition is observed. The qualitative agreement with the model predictions indicates the predictive power of the communicating walkers' model as well as the need to include repulsive chemotaxis signalling to capture the observed phenomena.

5.6. *Comment about universality*

In this section I have described the role of chemotactic interplay during complex patterning of the $\mathcal{T}$ morphotype. Is it a special ability of the $\mathcal{T}$ morphotype, or do other bacteria employ similar tactics for their adapative self-organization? I believe that these tactics are universal, and other bacteria such as *Bacillus circulans*, *E. coli*, *Salmonella*

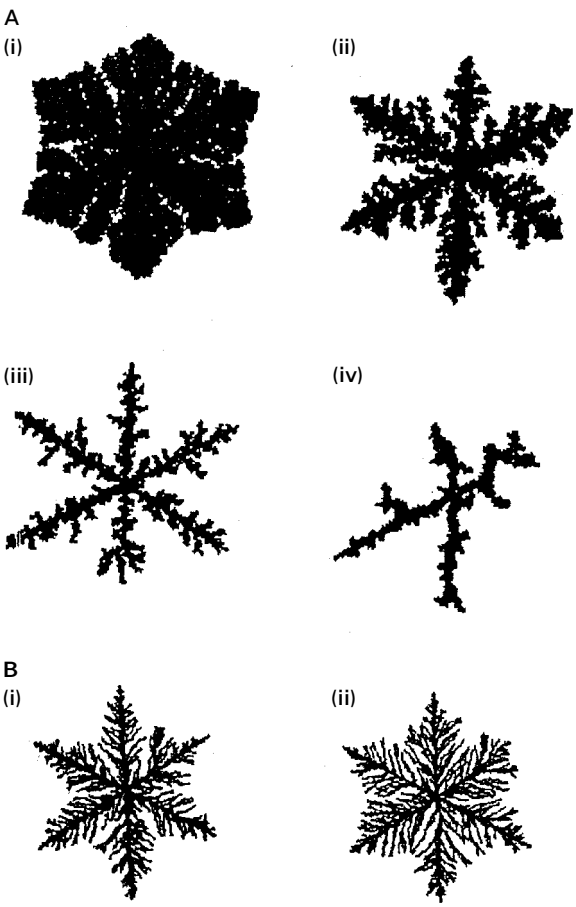

Figure 11. (a) Patterns produced by the 'communicating walkers' model in the presence of imposed sixfold anisotropy. The simulations are for N_c = 10. (*a*) (i) P = 50; (*a*) (ii) P = 20; (*a*) (iii) P = 10; (*a*) (iv) P = 5. At high levels of P the pattern is dense and the sixfold modulation is weak. At intermediate values of P the anisotropy is most pronounced. At very low values the patterns are ramified and the sixfold symmetry is lost. (*b*) The effect of repulsive chemotaxis. (*b*) (i) and (*b*) (ii) are the same as (*a*) (iv), but with repulsive chemotaxis (*b*) (i) is stronger than (*b*) (ii). The pattern becomes dense and the anisotropy is retained.

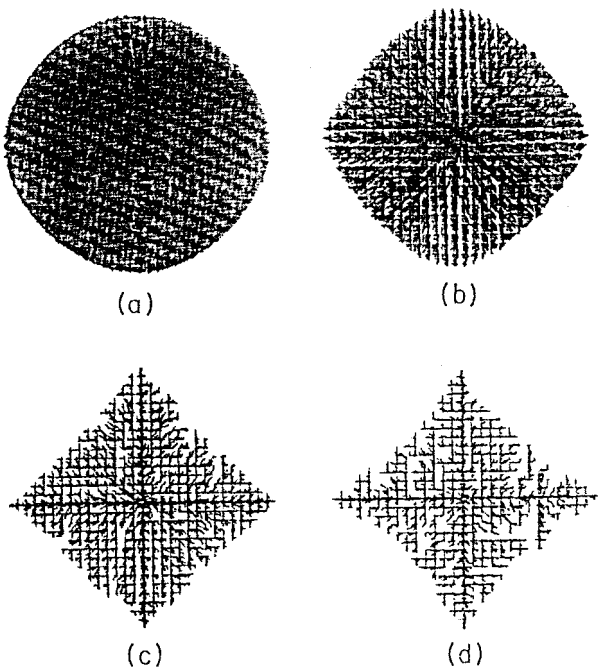

Figure 12. Patterns produced by the 'communicating walkers' model in the presence of fourfold lattice anisotropy and with repulsive chemotaxis signalling. The simulations are for N_c = 20. (*a*) P = 75; (*b*) P = 35; (*c*) P = 15; (*d*) P = 10. Note that the envelope shows a transition from concave shape to convex shape, as was shown in part I for a model of solidification from supersaturated solution.

typhimurium and *Proteus mirabilis* cope with hostile conditions in a similar manner, utilizing the interplay of long- and short-range chemotactic signalling for efficient self-organization. In [29, 73] we provide an explanation for

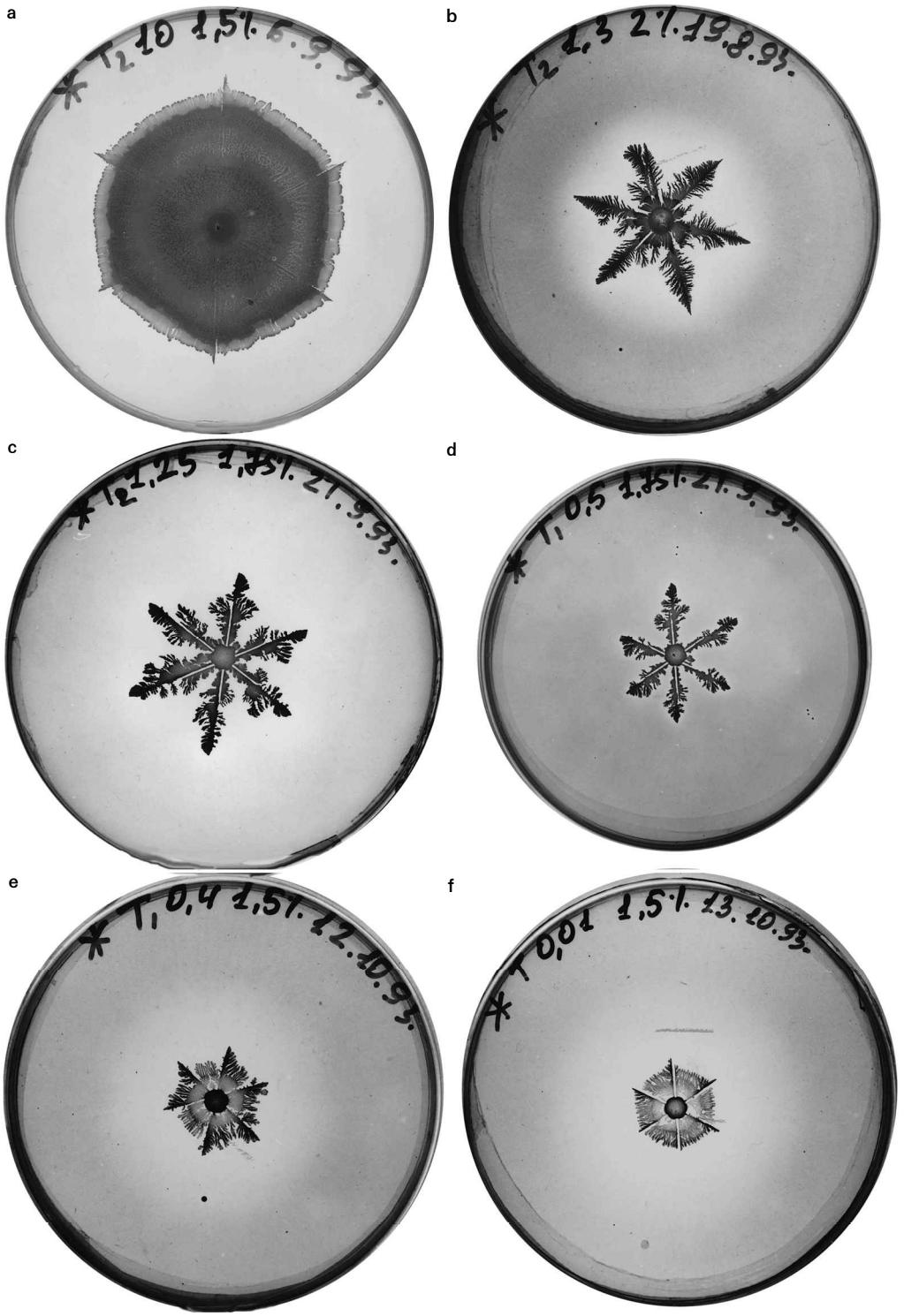

Figure 13. Grown 'bacterial snowflakes' for various peptone levels and agar concentrations respectively. (*a*) 10 g l^{-1}, 1.5%; (*b*) 1.3 g l^{-1}, 2%; (*c*) 1.25 g l^{-1}, 1.75%; (*d*) 0.5 g l^{-1}, 1.75%; (*e*) 0.4 g l^{-1}, 1.5; (*f*) 0.014 g l^{-1}, 1.5%.

patterning *E. coli* based on such an interplay. Here, in section 7, I show the crucial role of such tactics during colonial development of the vortex morphotype.

6. From flagella handedness to chiral patterns

Chiral asymmetry (first discovered by Louis Pasteur) exists in a whole range of scales, from subatomic particles

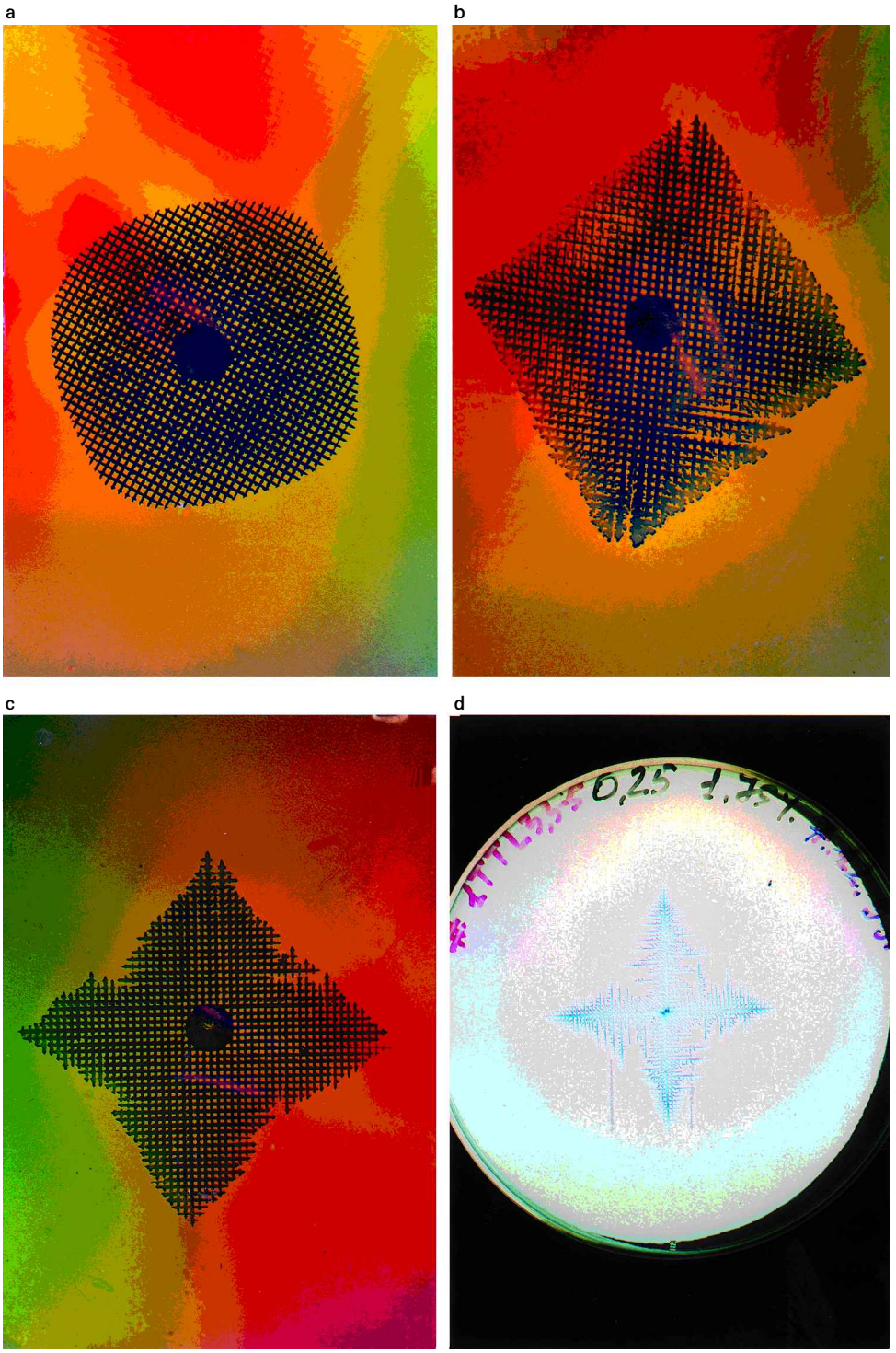

Figure 14. Patterns observed during growth in the presence of imposed fourfold lattice anisotropy for various peptone levels and agar concentrations respectively. (*a*) 10 g l^{-1}, 1.75%; (*b*) 4 g l^{-1}, 1.5%; (*c*) 1.4 g l^{-1}, 1.5%; (*d*) 0.25 g l^{-1}, 1.75%. Note the similarity to the model predictions shown in figure 12.

through human beings to galaxies, and seems to have played an important role in the evolution of living systems [75, 76]. Bacteria display various chiral properties. Mendelson and co-workers [33, 77–79] showed that long cells of *B. subtilis* can grow in helices, in which the cells form long strings that twist around each other. They have shown also that chiral characteristics affect the structure of the colony. We have found yet another chiral property: the strong chirality exhibited by the C morphotype. My purpose is to show that the flagella handedness, while acting as a singular perturbation, leads to the observed chirality. It does so in the same manner in which crystalline anisotropy leads to the observed symmetry of snowflakes (part I).

6.1. *Morphology diagram and a closer look at the patterns*

The C morphotype exhibits a wealth of different patterns according to the growth conditions (figure 15). As for the $\mathcal{T}$ morphotype, the observations may be organized in a morphology diagram and there is a velocity–pattern correlation [23]. Also, as for the $\mathcal{T}$ morphotype, the patterns are generally compact at high peptone levels and become ramified (fractal) at low peptone levels. At very high peptone levels and high agar concentrations, the C morphotype conceals its chiral nature and exhibits branching growth similar to that of the $\mathcal{T}$ morphotype.

Optical microscopy observations indicate that during growth of strong chirality the cells move within a well defined envelope. The cells are long relative to those of the $\mathcal{T}$ morphotype, and the movement appears correlated in orientation. Each branch tip maintains its shape, and at the same time the tips keeping twisting with specific handedness while propagating. Electron microscopy observations do not reveal any chiral structure on the cellular membrane [28].

6.2. *The riddles*

In the introduction I mentioned the transitions between the $\mathcal{T}$ and the C morphotypes. During growth on soft substrate (about 1% agar concentration), about 60% of $\mathcal{T}$ morphotype *colonies* show bursts of the C morphotype (figure 16). The reverse $C \rightarrow \mathcal{T}$ transitions are observed during growth of C morphotype colonies on hard agar (figure 16). On soft agar the colonies of C morphotype grow faster than colonies of $\mathcal{T}$ morphotype, and vice versa on hard agar. Hence the transitions are to the faster-growing morphotype. Since the growth velocity is a colonial property, it seems as if some colonial selection pressure acts towards higher growth velocity. Such a principle would be an extension to living systems of the 'fastest-growing morphology' selection principle that we proposed for non-living systems.

Now we are facing several riddles. One is the manner in which colonial selection pressure can reach down and cause genetic changes in the individual cells (and transform them between $\mathcal{T}$ and C). Another riddle concerns the morphotype bursts. For example, sparse cells of the C morphotype scattered among the $\mathcal{T}$ cells have no individual advantage and no effect on the colony structure; only a finite nucleation of the C cells has an advantage on soft agar, as they can develop a part of the colony that overgrows the original $\mathcal{T}$ morphotype [22, 23]. The question is then how finite nucleation is formed. In [22, 23] we raised the possibility of autocatalytic or cooperative genetic transformations. Another option might be a special response of the C cells to a chemotactic agent emitted by the $\mathcal{T}$ cells, that may, for example, cause them to move faster and aggregate.

A third riddle has to do with the biological property of the individual cells that leads to chiral patterning. Being frequent and in both directions, it is suggestive that the $\mathcal{T} \rightleftharpoons C$ transitions are associated with activation and deactivation of a biological property which is simple yet capable of causing the dramatic changes in the growth patterns. From the microscope observations it seems that the significant change on the scale of the individual cell is in the length – the C cells are longer. We wonder what the connection is between cells' lengths and the formation of chiral patterns. In this section, I describe a plausible solution to that. The former two riddles are still open, but there are indications that their solutions may lead to a very exciting new biological understanding, as I suggest in section 8.

6.3. *Proposed mechanism based on flagella handedness*

It is known [56, 80, 81] that flagella have specific handedness. We propose that the latter is the origin of the observed chirality [30]. In a fluid (which is the ordinary state under study), as the flagella unfold, the cell tumbles and ends up at a new random angle relative to the original one. The situation changes for quasi-two-dimensional motion, motion in a 'lubrication' layer thinner than the cellular length. We assume that, in this case of rotation in a plane, the tumbling has a well defined handedness of rotation. Such handedness requires, in addition to the chirality of the flagella, the cells' ability to distinguish up from down. The growth in an upside-down Petri dish shows the same chirality. Therefore we think that the determination of up as against down is done via either the vertical gradient of the nutrients concentration or the vertical gradient of signalling materials inside the substrate or the attachment of the cells to the surface of the agar.

To cause the observed chirality, the rotation of tumbling must be, on average, less than 90° and relative to a specific direction. We assume that in the case of long cells, like the C morphotype, a cell–cell co-alignment (orientation interaction) limits the average rotation. We further assume that

the rotation is relative to the local mean orientation of the surrounding cells.

6.4. *Modelling the new mechanism*

To test the above idea, we included the additional assumed features in the communicating walkers' model [27]. As before, the bacterial cells are represented by walkers, each of which should be viewed as a mesoscopic unit, but in this case each walker represents only 10 – 1000 cells. Again the metablic state of the ith walker (located at $\mathbf{r}_i$) is represented by an 'internal energy' E_i. The time evolution of E_i, food consumption and food diffusion are the same as described in section 4 for the $\mathcal{T}$ morphotype.

To represent the cellular orientation we assign an angle θ_i to each walker. Every time step, each of the active walkers ($E_i > 0$) performs rotation to a new orientation θ'_i, which is derived from the walker's previous orientation θ_i by

$$\theta'_i = P(\theta_i,\ \Phi(\mathbf{r})_i)) + Ch + \xi, \tag{12}$$

where Ch and ξ represent the new features of rotation due to tumbling. Ch is a fixed part of the rotation and ξ is a stochastic part, chosen uniformly from the interval $[-\eta, \eta]$. $\Phi(\mathbf{r}_i)$ is the local mean orientation in the neighbourhood of $\mathbf{r}_i$. P is a projection function that represents the orientational interaction which acts on each walker to orient θ_i along the direction $\Phi(\mathbf{r}_i)$. P is defined by

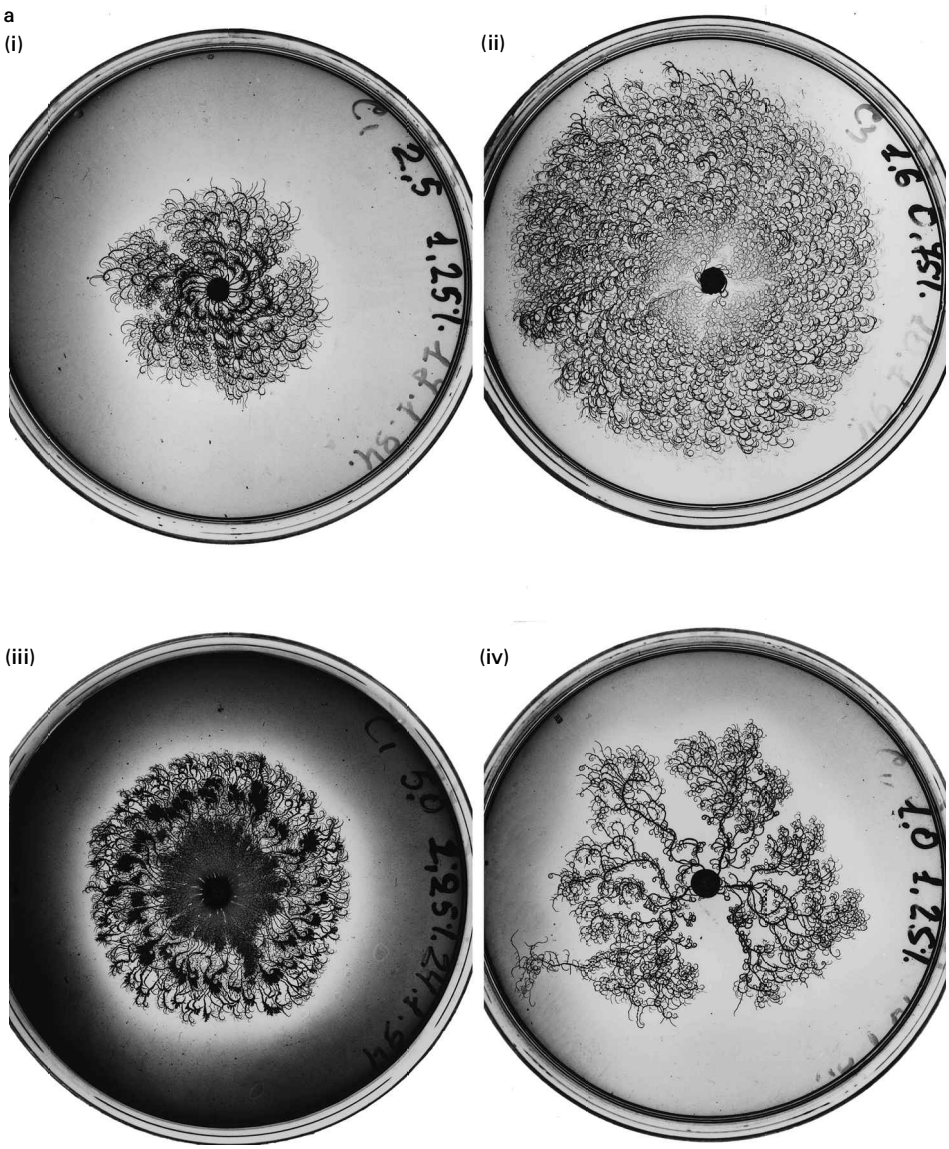

$$P(\alpha,\beta) = \alpha + (\beta - \alpha) \bmod \pi. \qquad (13)$$

Once oriented, the walker advances a step d either in the direction θ'_i (forwards) or in the direction $\theta'_i + \pi$ (backwards). Hence the new location $\mathbf{r}'_i$ is given by

$$\mathbf{r}'_i = \mathbf{r}_i + \begin{cases} d(\cos\theta'_i, \sin\theta'_i), & \text{with probability 0.5,} \\ d(-\cos\theta'_i, -\sin\theta'_i), & \text{with probability 0.5.} \end{cases}$$

As for the $\mathcal{T}$ morphotype, the movement is confined within an envelope which is defined on a triangular lattice. The step is not performed if $\mathbf{r}'_i$ is outside the envelope. Whenever this is the case, a counter on the appropriate segment of the envelope is increased by one. When a segment counter reaches N_c, the envelope advances one lattice step and a new lattice cell is occupied.

Next we specifiy the mean orientation field Φ. To do so, we assume that each lattice cell (hexagonal unit area) is assigned one value of $\Phi(\mathbf{r})$, representing the average orientation of the cells in the local neighbourhood. The value of Φ is set when a new lattice cell is first occupied owing to the advancement of the envelope and then remains constant. We simply set the value of Φ equal to

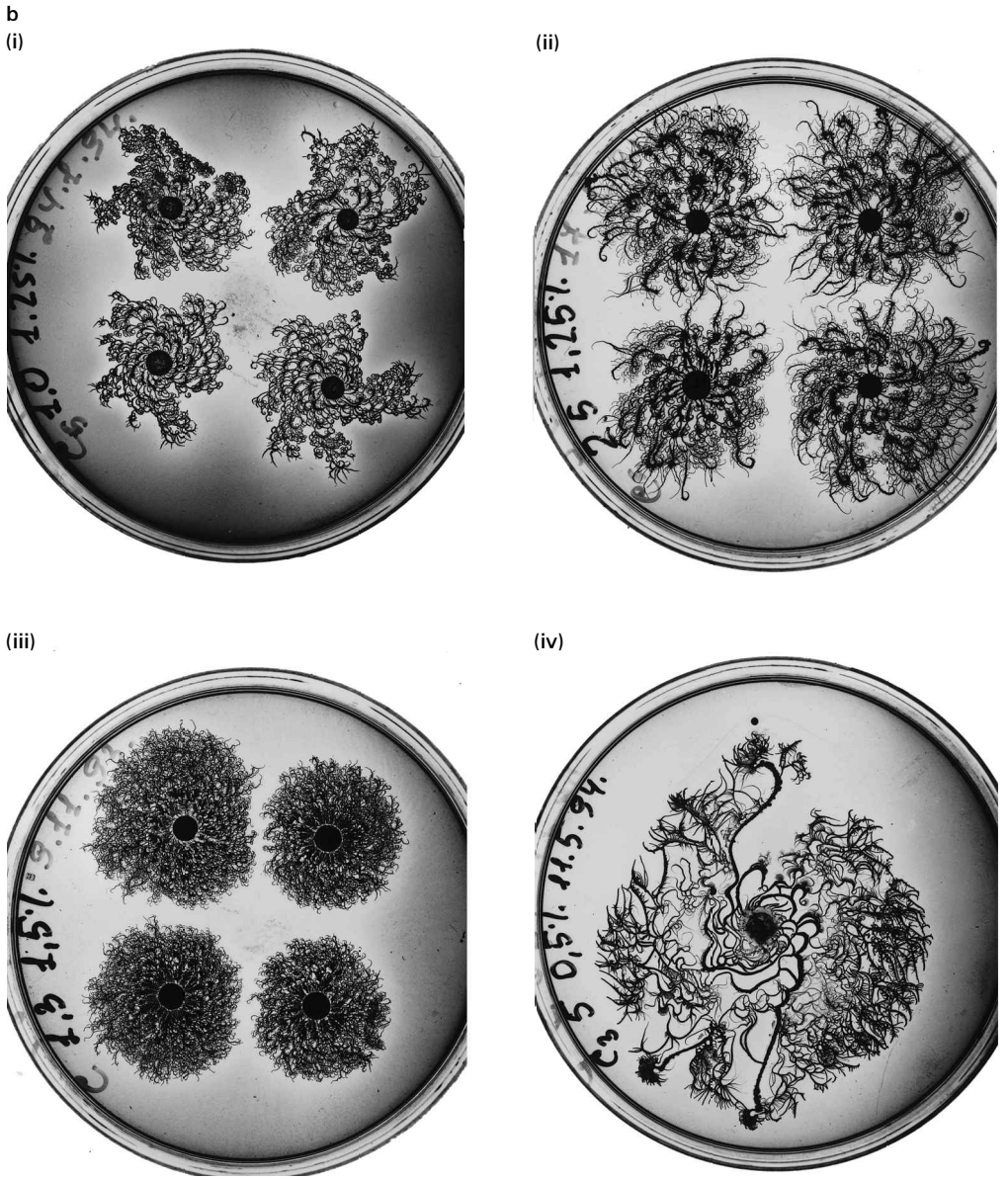

Figure 15. Examples of patterns developed by colonies of the *C* morphotype grown in different conditions, i.e. for various pepton levels and agar concentrations respectively; (*a*) (i) 2.5 g l^{-1}, 1.25%; (*a*) (ii) 1.65 g l^{-1}, 0.75%; (*a*) (iii) 5.0 g l^{-1}, 1.25%; (*a*) (iv) 1.0 g l^{-1}, 1.25%; (*b*) (i) 1.0 g l^{-1}, 1.25%; (*b*) (ii) 2.5 g l^{-1}; 1.25%; (*b*) (iii) 1.3 g l^{-1}, 1.5%; (*b*) (iv) 5.0 g l^{-1}, 0.5%.

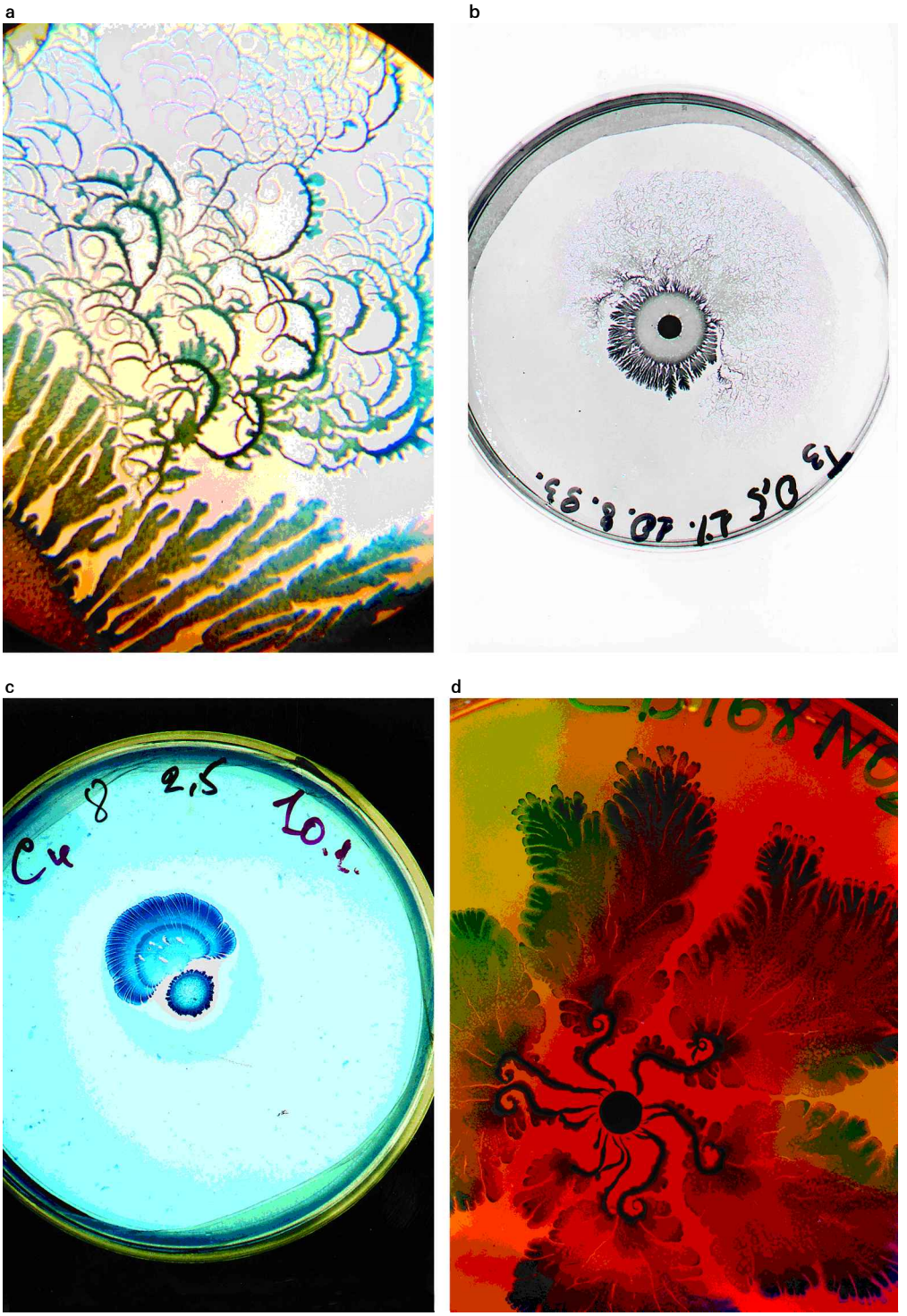

Figure 16. $\mathcal{T} \rightleftharpoons C$ transitions. (*a*), (*b*) transitions from $\mathcal{T}$ to C during growth at an agar concentration of 1% and a peptone level of 5 g l^{-1}. Note that for these growth conditions the C morphotype spreads much faster than the $\mathcal{T}$ morphotype. (*c*) The reverse $C \rightarrow \mathcal{T}$ transition at an agar concentration of 2.5% and peptone level of 8 g l^{-1}. For these growth conditions the $\mathcal{T}$ is the faster morphotype. The C morphotype does not show the chiral pattern but a compact growth. (*d*) Phenotypic tip-splitting growth exhibited by C morphotype at a high peptone level.

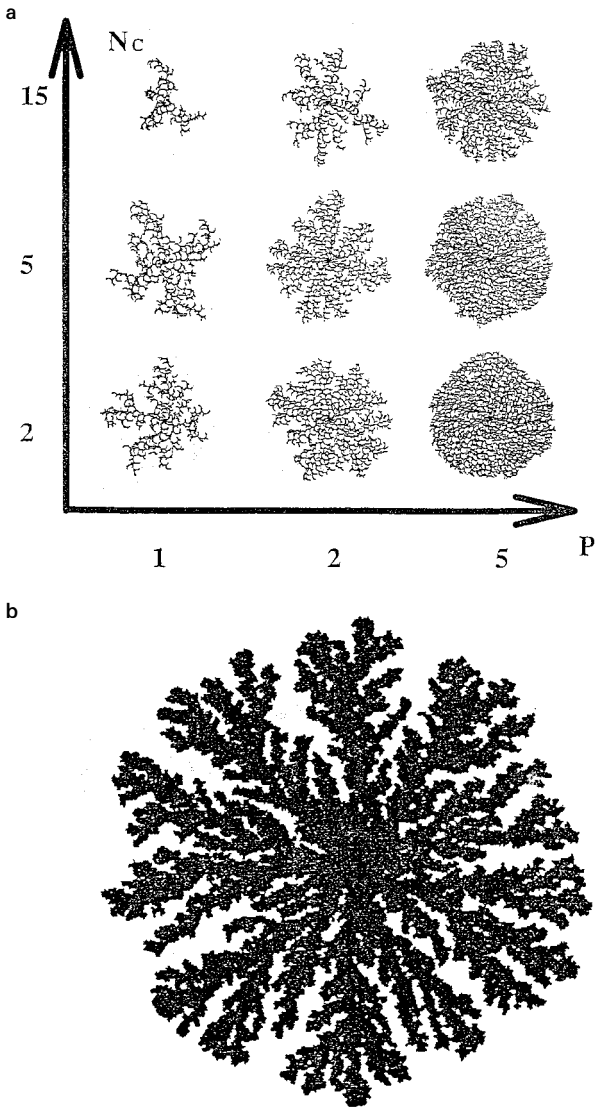

Figure 17. Results of numerical simulations of the model for *C* morphotype described in the text. (*a*) Chiral patterns for $\xi = 3$. (*b*) Tip-splitting growth for large noise ξ. *P* and N_c are the peptone level and agar concentration as explained in figure 6. Note the similarity to the observed pattern shown in figure 4 (*b*).

the average over the orientations of the N_c attempted steps that lead to the occupation of the new lattice cell. Clearly, the model described above is a simplified picture of the cell's movement. For example, a more realisitc model will include an equation describing the time evolution of Φ. However, the simplified model is sufficient to demonstrate the formation of chiral patterns.

Results of the numerical simulations of the model are shown in figure 17. These results do capture some important features of the observed patterns; the microscopic twist *Ch* leads to a chiral morphology on the macroscopic level. The growth is via stable tips, all of

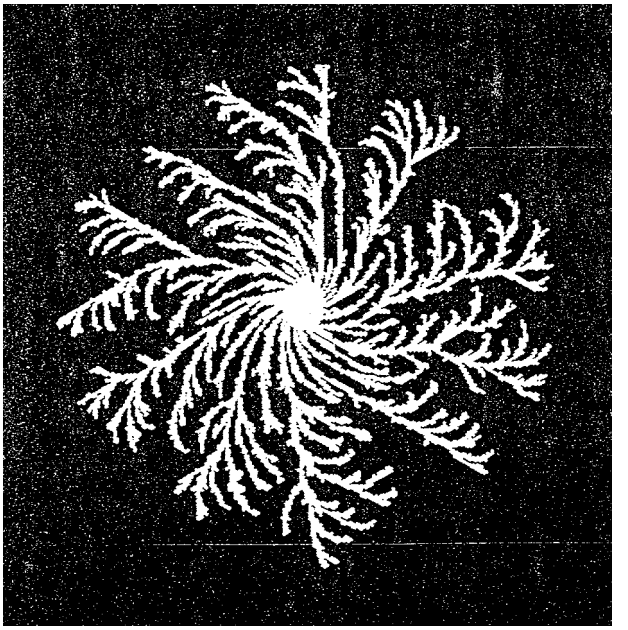

Figure 18. Simulations of weak chirality as explained in the text.

which twist with the same handedness and emit side branches. The dynamics of the emission of side branches in the time evolution of the model is similar to the observed dynamics.

For large noise strength η the chiral nature of the pattern gives way to a branching pattern (figure 17). This provides a plausible explanation for the branching patterns produced by the *C* morphotype grown at high peptone levels (figure 16), as the cells are shorter when grown on a rich substrate. The orientation interaction is weaker for shorter cells, and hence the noise is stronger.

6.5. *Plausible explanation of weak chirality*

In figure 3 we show a pattern of weak chirality exhibited by the $\mathcal{T}$ morphotype colonies grown on a hard substrate. We propose that, in the case of the $\mathcal{T}$ morphotype, it is the high viscosity of the 'lubrication' fluid during growth on a hard surface that replaces the cell–cell co-alignment of the *C* morphotype that limits the rotation of tumbling. We further assume that the rotation should be relative to a specified direction. The gradient of chemotaxis signalling field (here we used repellent chemotaxis) serves as a specific direction, rather than the local mean orientation field in the case of the *C* morphotype. In figure 18 we show that inclusion of the above features indeed leads to a weak chirality which is highly reminiscent of that observed. The idea above also provides a plausible explanation to the observations of weak chirality by Matsuyama and Matsushita [26] in strains defective in production of 'lubrication' fluid.

a

(i)

(ii)

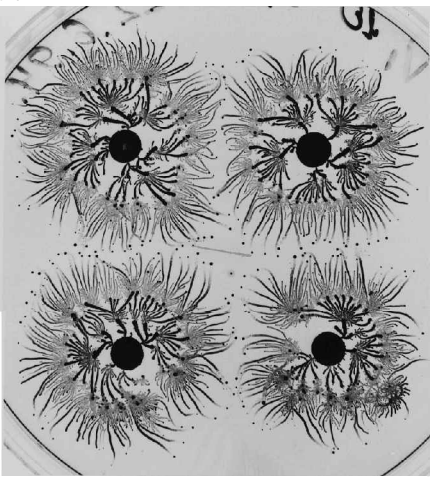

(iii)

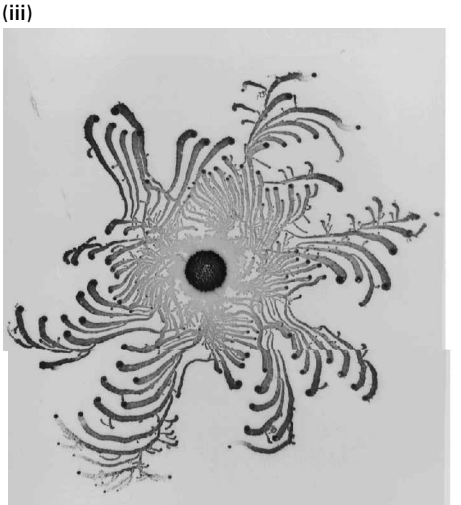

(iv)

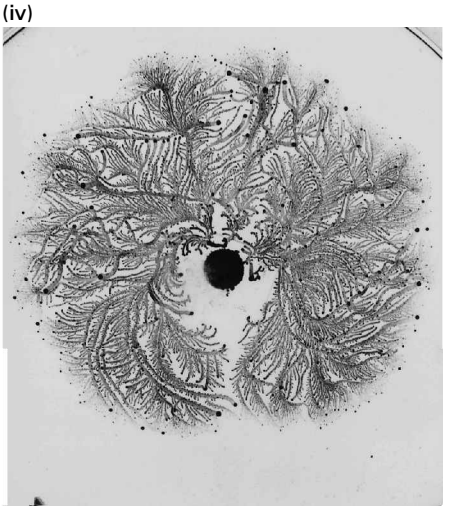

(v)

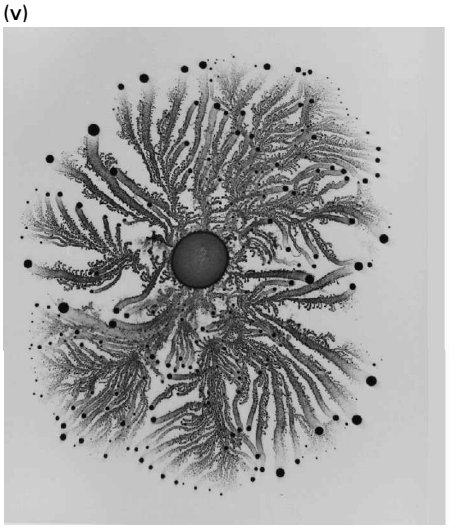

(vi)

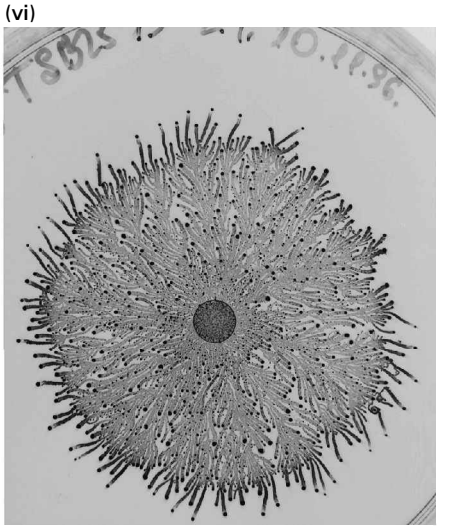

6.6. *A search for a new mechanisms of chemotactic response*

So far I have described the proposed explanations of the observed strong chirality of the *C* morphotype, its ability to develop branching patterns (on hard substrate and high levels of peptone) and the weak chirality exhibited by the $\mathcal{T}$

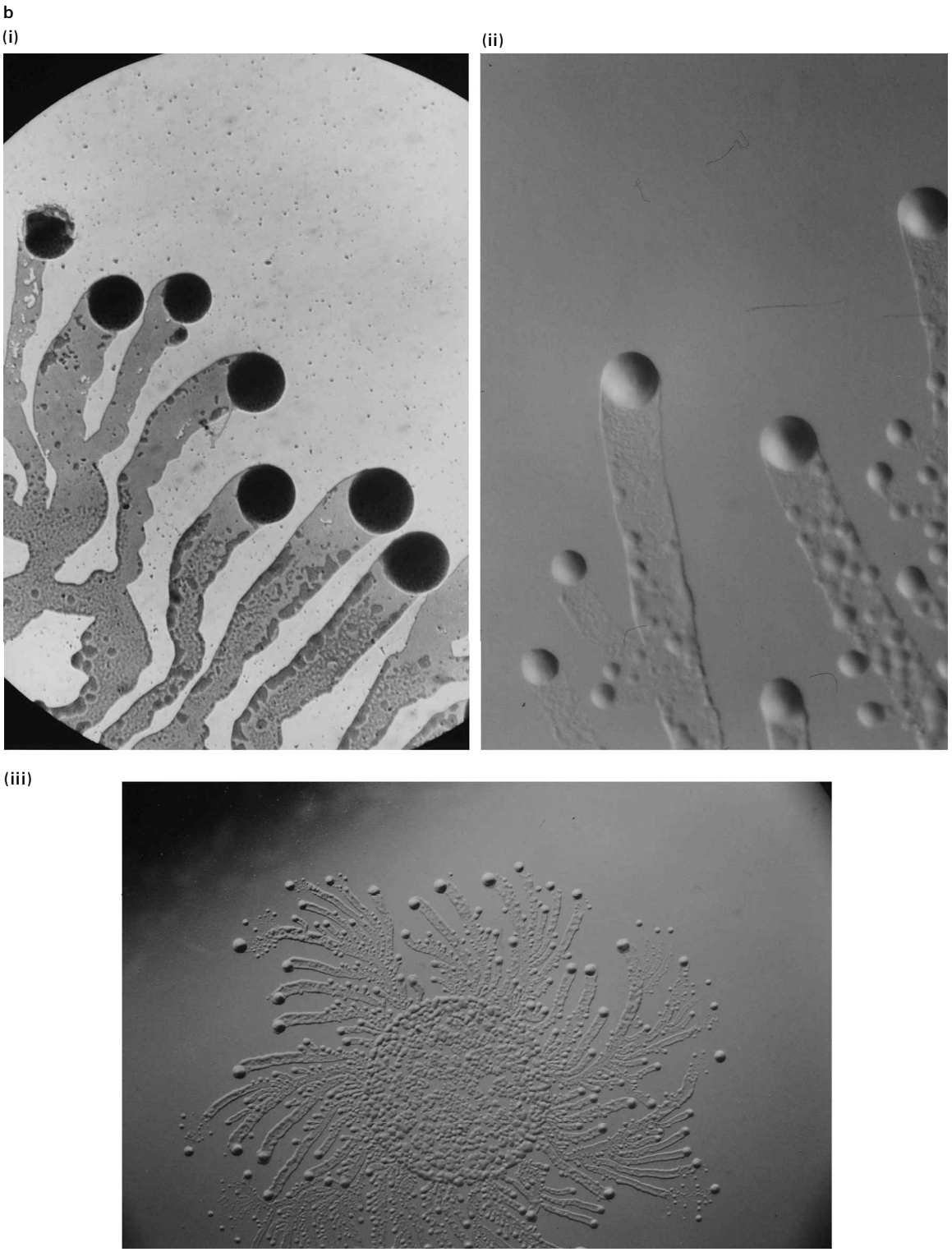

Figure 19. Patterns developed by colonies of the $\mathcal{V}$ morphotype. (*a*) (i) 15.0 g l^{-1}, 2.25%; (*a*) (ii) 10.0 g l^{-1}, 2.25%; (*a*) (iii) 5 g l^{-1}, 2.25%; (*a*) (iv) 3 g l^{-1}, 2.5%; (*a*) (v) 2.5 g l^{-1}, 2.5%; (*a*) (vi) 15 g l^{-1}, 2%. (*b*) Closer look at the vortices.

morphotype (on hard substrate). These are only few of the observed phenomena. Colonies of $\mathcal{C}$ morphotype exhibit a profusion of patterns. Some are shown in figure 15, but there are many more. Additional features must be included in the model to reproduce the observed patterns. Keeping the idea of universal tactics, it is tempting to include some mechanisms of chemotactic response. Clearly, they must differ from the mechanisms employed by the $\mathcal{T}$ morphotype. As explained in section 3, in the case of tumbling bacteria, the average movement is biased up or down the gradient as tumbling is delayed when an increase or decrease in concentration is detected, and thus attractive or repulsive chemotaxis is implemented.

The way that a chemotactic response is implemented in the $\mathcal{C}$ morphotype is still an open question to be studied in the future. As we have seen, the length of the cells plays a crucial role in the formation of the chiral patterns. It might be that the $\mathcal{C}$ morphotype bacteria also employ chemoregulation of their length. Again, this possibility is left for future studies.

7. Formation of vortices by gliding and swarming bacteria

Vortices are formed in many natural systems, ranging from the oceans and atmosphere (e.g. tornadoes, hurricanes and the famous 'eye' on Saturn) to superconductors and superfluids. Vortices may also be formed by schools of organisms; a well known example is the circular flight of flocks of birds in rising hot air. The vortices are topological collective excitations of the system in which there is a correlated radial motion around a common centre. In a simple rigid vortex the velocity is proportional to the distance from the centre. The vortices may have an internal structure, typically a motionless core. In the study of the vortex dynamics, the vortices themselves are sometimes viewed as interacting particles (each vortex is one particle). Indeed, the interaction between the vortices can lead to self-organization, for example vortex lattice in type II superconductors.

Observations of vortices formed by bacterial colonies of *B. circulans* have been reported [82–84] more than half a century ago. Vortices are only one of the phenomena produced by the *B. circulans*. They also exhibit collective migration, 'turbulent-like' collective flow, complicated vortex dynamics including merging and splitting of vortices, attraction and repulsion, etc., rotating 'bagels' and more. A fascinating movie of the *B. circulans* [84] shows some of those phenomena and ends with a remark that the observed phenomena might be too complicated for them ever to be explained. Indeed, even the simplest phenomena of collective migration of schools of organisms have posed a challenge for many years. Only recently have satisfying models been devised (for example [85, 86]).

During our studies of complex bacterial patterning, new strains which exhibit similar behaviour to *B. circulans* were isolated [21, 23, 87]. We refer to these new strains as $\mathcal{V}$ (vortex) morphotype, as their most noticeable character is their ability to form vortices. I describe here experimental observations of the migration dynamics and colony patterns exhibited by the $\mathcal{V}$ morphotype. These bacterial cells exhibit similar dynamics to that of the *B. circulans*. A close study of these observations enabled us to construct a model of colonial development applicable for both gliding and swarming bacteria.

7.1. *Bacterial patterns and dynamics*

A wide variety of patterns are exhibited by the $\mathcal{V}$ morphotype as the growth conditions are varied. Some representative patterns are shown in figure 19. Each branch is produced by a leading droplet of cells and emits side branches, each with its own leading droplet. In many cases the branches have a well pronounced global twist.

Each leading droplet consists of several to millions of cells that rotate around a common centre (hence the term vortex) at a typical cell speed of 10 μm s^{-1}. Both the size of a vortex and the speed of the cells can vary according to the growth conditions and the location in the colony. Futhermore, within a given colony, both clockwise and anticlockwise rotating vortices are observed. The vortices in a colony can also consist of either a single layer or multiple layers of cells. We occasionally observed vortices with an empty core or 'bagel' shaped. After formation, the number of cells in the vortex increases, the vortex expands and translocates as a unit. The speed of the vortices as units is slower than the speed of the individual cells circulating around the centre.

Bacterial cells are also contained in the trails left behind the leading vortices. Some are immobile while others move, swirling with complex dynamics; groups containing a few to thousands of cells move in various directions, changing direction abruptly and sometimes returning to a previous location. Occasionally, two such groups pass by each other and unite into a single group, or they might remain separate despite the close contact. Quite often, groups of cells are reminiscent of the 'worm' motion of slime mould or schools of multicellular organisms.

Microscopic observations of the $\mathcal{V}$ morphotype reveal that the cells perform a collective motion very much like that of a viscous fluid. We observe neither tumbling nor movement forwards and backwards. Rather, the motion is always forwards, and the cells all tend to move in the same direction and speed as the surrounding cells, in a synchronized group. Electron microscopy observations show that the bacteria have flagella, which indicates that the movement is swarming [32]. The whole intricate dynamics are confined to the trail of the leading vortices,

and neither a single cell nor a group of moving cells can pass the boundary of the trail. Only vortices formed in the trails can break out and form a new branch.

7.2. *Modelling the collective migration*

To model gliding and swarming bacteria we follow the communicating walkers' model, but now cells are represented by gliders instead of walkers [31]. Each glider is characterized by both its location $\mathbf{r}_i$ and its velocity $\mathbf{v}_i$. The equation describing the change in the glider's position is simply

$$\frac{\mathrm{d}\mathbf{r}_i}{\mathrm{d}t} = \mathbf{v}_i. \tag{14}$$

The description of the velocity change is more intricate:

$$\frac{\mathrm{d}\mathbf{v}_i}{\mathrm{d}t} = \Gamma \frac{\mathbf{v}_i}{|\mathbf{v}_i|} - \nu\mathbf{v}_i + \mu(\langle\mathbf{v}\rangle_{i,\epsilon} - \mathbf{v}_i) - \chi_\sigma \nabla\sigma + \xi. \tag{15}$$

The terms on the right-hand side of Equation (15) are as follows: firstly the propulsion force Γ of the glider, which acts in the direction of $\mathbf{v}_i$; secondly the frictional force with the surroundings with a friction coefficient ν (these first two terms tend to set the glider's speed of Γ/ν); thirdly velocity – velocity interactions which leads to alignment of the velocity with the neighbours' mean velocity $(\mathbf{v})_{i,\epsilon}$ averaged over a radius ϵ; fourthly a hard-core interaction term, which leads to a repulsion of the glider from regions of high glider density (the local density of the gliders is denoted by σ); fifthly a term representing all other unknown factors, approximated by a random force ξ (we emphasize that this term is included to demonstrate that the dynamics of the model are not sensitive to noise).

In reality, the coefficient Γ, μ and ν of Equation (15) depend on the local amount of extracellular wetting fluid. In the model this feature is included by the fact that a glider can move only if the level of extracellular wetting fluid w in its vicinity is larger than a threshold value W. Each glider carries an amount of fluid s_i and releases it as slime if the surface is dry ($w(\mathbf{r}_i) < W' < W$). When a glider encounters a place where w is below W (i.e. the colony boundary), it is reflected from the boundary where it deposits fluid.

The above features are sufficient to capture the cellular collective migration. For a given level of noise and sufficiently high density of cells, the velocities align and the cells perform a collective migration. What is still missing is the additional features that cause vortices to emerge out of the collective migration.

7.3. *Rotational chemotaxis and vortex formation*

It has previously been shown [31, 88, 89] in a related model that geometrical constraints of reflecting boundaries can lead to circular collective motion. This result suggests that a radial inward 'force' can lead to vortex formation. We proposed [32, 90, 91] in this regard that a new chemotactic response to a self-emitted attractant provides such an inward 'force'.

In the case of tumbling bacteria, the average movement is biased up or down the gradient, as tumbling is delayed when an increase or decrease in concentration is detected, and thus attractive or repulsive chemotaxis is implemented [62]. Clearly, a different strategy of chemotactic response is required in the case of gliding or swarming bacteria that do not tumble. We propose that in this case the individual cells weakly vary the propulsion force according to the local concentration of a chemomodulating agent. For high concentrations of the chemical, the force is decreased for an attractive response or increased for a repulsive response. Such a response creates a gradient of propulsion force Γ in a group of cells moving together. Combined with the velocity – velocity interaction, this imposes a torque or local vorticity on the average motion of the cells. Therefore a glider moving at an angle to the chemical gradient is subjected to a torque which causes the glider to twist towards the direction of the local gradient of the chemoattractant. The term describing such an attractive rotational chemotactic response is described by

$$-\chi_\mathrm{A} \frac{1}{v_i}(\mathbf{v}_i \times \nabla C_\mathrm{A}), \tag{16}$$

where C_A is the concentration of the attractant and χ_A is a pre-factor, which is a measure of the sensivity to the chemomodulator. This term should be added to the right-hand side of equation (15), and Γ should vary in space according to C_A. The time evolution of C_A is described by a diffusion equation similar to equation (9) without decomposition by walkers ($\Omega_\mathrm{A} = 0$). The rotational chemotaxis produces the force required to keep the cells circulating. In figure 20 we show vortices formed in numerical simulations of the model, when emission of attractant and rotational chemotactic response are included.

7.4. *Modelling the cooperative organization of colonies*

We have shown that chemomodulation can indeed lead to the formation of stationary vortices (fixed in size and location), rotating 'bagels' (figure 20) and other elements. All these elements are of a length scale comparable with or smaller than an individual branch of a colony. During colonial development, these elements are organized to form the observed global pattern.

When modelling colony formation, we must remember that bacterial cells in a colony do not move in a predetermined space, and that their number and state of activity are not conserved. While the colony expands and changes its shape, cells reproduce and sporulate. To provide the means for reproduction, movement and other

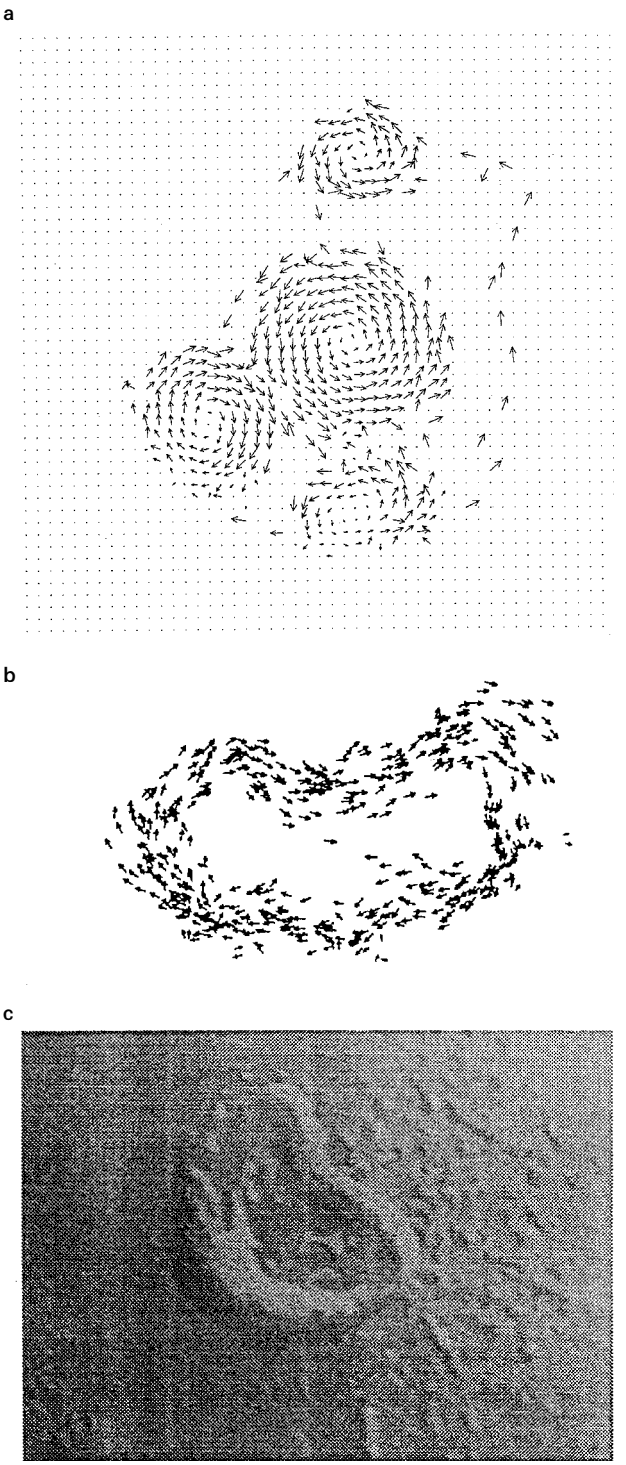

Figure 20. Numerical simulations of the 'communicating gliders' model for the $\mathcal{V}$ morphotype, with the inclusion of attractive rotational chemotaxis. The arrows indicate the direct and magnitude of the gliders' velocity. We started the simulations with randomly scattered gliders which have random velocities. (*a*) Spontaneous formation of vortices. (*b*) Formation of a 'bagel'-like pattern. (*c*) Close picture of an observed 'bagel'.

metabolic processes, the cells consume nutrients from the environment.

Again we represent the metabolic state of the ith glider by an 'internal energy' E_i, the rate of change of which is given by equation (6). The diffusion of nutrients is also modelled as in the communicating walkers' model.

Additional features are employed by the colony to provide the required control and regulation mechanisms for efficient self-organization. Motivated by our studies of other morphotypes, we assume that a kind of chemorepellent is employed, whose characteristic length scale is longer than the diameter of an individual vortex. Hence it is capable of regulating the movement of the vortices, each as an individual unit. Such a mechanism is required in order to avoid locking of the vortices in place by the self-emitted attractant.

The time evolution of the repellent C_R is the same as that of R in equation (11) (in the stimulation below there was no decomposition by the walkers $\Omega_R = 0$). The effect of the repellent on the glider movement is represented by a term similar to equation (16) but opposite in sign. After the inclusion of both the chemoattractant and the chemorepellent terms, equation (15) becomes

$$\frac{d\mathbf{v}_i}{dt} = \Gamma \frac{\mathbf{v}_i}{vi} - v\mathbf{v}_i - (-\chi_\sigma \nabla\sigma) + \mu(\langle \mathbf{v} \rangle_{i,\epsilon} - \mathbf{v}_i) - \frac{1}{v_i}\mathbf{v}_i \times [\mathbf{v}_i \times (\chi_A \nabla C_A - \chi_R \nabla C_R] + \xi, \qquad (17)$$

We assume that the repellent material decays slowly, so that its concentration C_R is almost constant over distances comparable with the typical size of a vortex (long-range chemotaxis). This is in contrast with the attractant concentrations which is assumed to vary considerably within a vortex (short-range chemotaxis). Thus, although the functional form of the repulsion term is similar to that of the attraction term, it has a different effect on the bacterial motion. It affects each vortex as a single unit and provides a mechanism for regulating colony structure during colonial development. On each vortex, the repulsion acts effectively as a combination of centrifugal and Lorentz forces (relative to the centre of the colony, and not of the vortex) pushing the vortices outwards on curved trajectories. In figure 21 we show results of numerical simulations where both long-range repulsive and short-range attractive chemotaxis are included. Microscopy observations reveal the presence of cells left behind the vortices. Therefore we also included in the simulations a finite probability that the gliders become immobile.

7.5. *Spiral patterns*

It is tempting to suggest that variations in the model presented here can be applied to studying the behaviour of other species of gliding and swarming bacteria. For

example, the concept of rotational chemotaxis could be invoked to explain the observed collective migration of gliding *Myxobacteria* towards food sources [5]. In this regard it will be of interest to determine whether *Myxobacteria* can form vortices under suitable growth conditions, such as harder agar surfaces. The generality and the advantages of vortex formation by gliding and swarming bacteria remain to be determined.

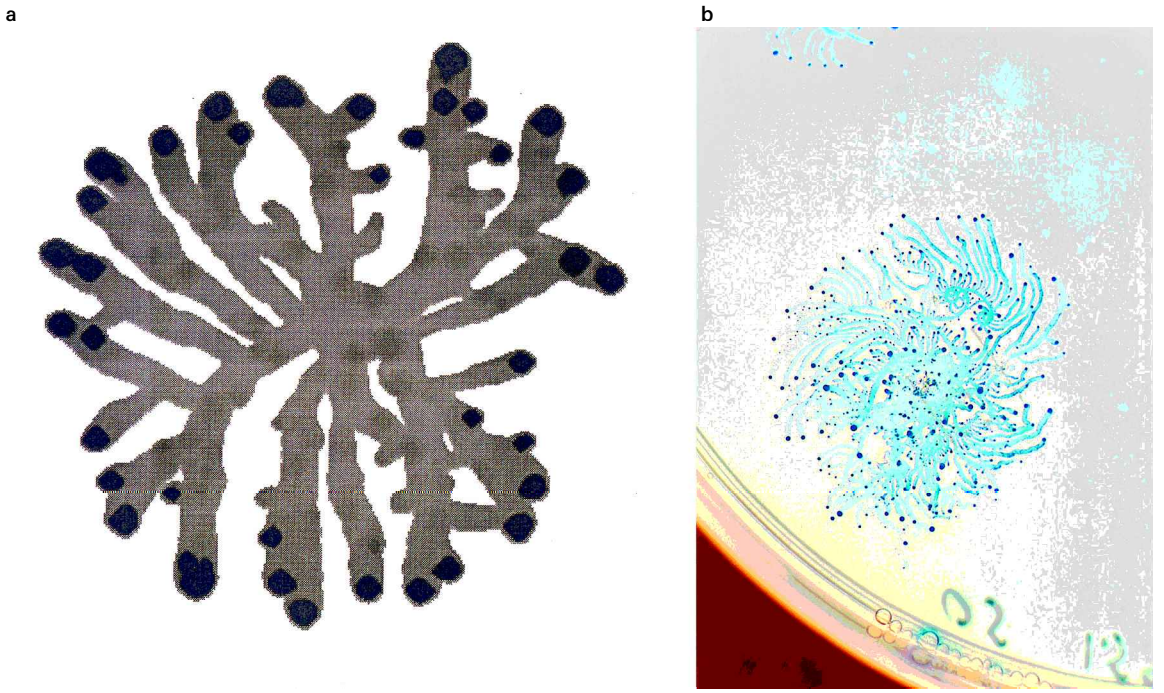

Figure 21. (*a*) **Simulations of colony development. Both repellent and attractant rotational chemotaxis are included, as well as food diffusion, reproduction, sporulation and production of wetting fluid.** (*b*) **Examples of an observed colony.**

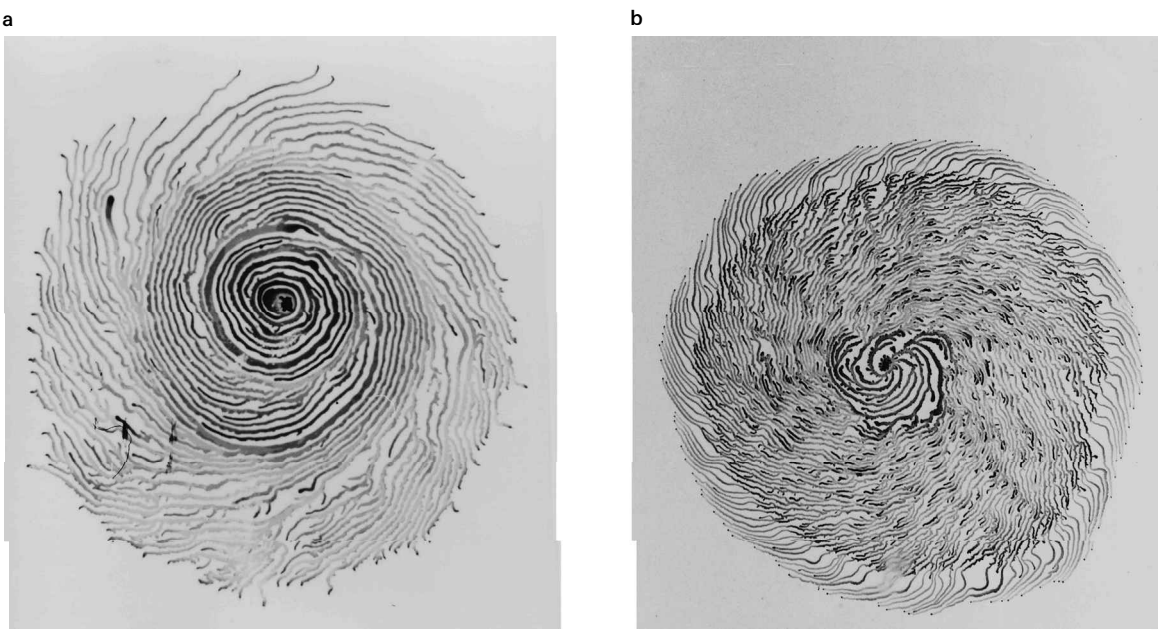

Figure 22. Patterns developed by colonies of the SV morphotype. Growth conditions: peptone level, 2 g l^{-1}; agar concentration, 1.5%. (a) one of 5 colonies grown on the Petri dish. (b) a single colony grown on the Petri dish

Recently we have isolated from the $\mathcal{V}$ morphotype a new strain which poses a challenge to the predictive power of the modelling approach. The new strain exhibits spectacular macroscopic spiral formations (figure 22), and hence we named it $S\mathcal{V}$ (spiral vortex). Under the microscope it is revealed that the droplets leading the branches are sometimes vortices, but not always. Sometimes a branch is led by a droplet of cells which does not spin but only moves forwards slowly. Another feature displayed by the $S\mathcal{V}$ morphotype is 'worms' in the interior of the colony that perform strikingly fast (much faster than the leading droplets) motion, over 100 μm s^{-1}. Such a group moves in an almost straight line over long distances, then stops, sometimes spins for a while and then moves in a new direction. In some cases these 'worms' merge with a 'well behaved' vortex; in other cases they are 'created' as a vortex splits into two.

We believe that a variation in the present model can explain the spiral pattern. One possibility is that the spiral nature of the colony results from non-monotonic response to the chemorepellent, which tends to 'lock' groups movement at a certain concentration of chemorepellent. At high gradients, such response can also disrupt the order imposed by the chemoattractant and prevent the formation of vortices. Clearly, future experimental and theoretical studies are required to find out whether this is the right explanation.

8. Conclusions

It is now understood that bacteria paved the way for life on Earth as we know it and are crucial for its continuation. Yet the view of bacteria as unicellular microbes — or a collection of non-interacting passive 'particles' — has persisted for generations. Only recently has the notion of 'bacteria as multicellular organisms' been put forward [5, 58, 92]. Shapiro [5] concluded his 1988 paper saying: 'Although bacteria are tiny, they display biochemical, structural and behavioural complexities that outstrip scientific description'.

We saw some striking complex patterns forming during colonial development of several bacterial strains at a variety of environmental conditions. These patterns reflect self-organization of colonies which is required for efficient adaptation to adverse growth conditions. Efficient self-organization can only be achieved through cooperative behaviour of the individual cells. Invoking ideas from pattern formation in non-living systems and using generic modelling, we were able to correlate the patterns with sophisticated strategies of cooperation employed by the bacteria. To achieve the required level of cooperation the bacteria have developed various communications capabilities. Here we specifically included the following: firstly direct cell–cell interactions leading to the orientational interactions of the C morphotype and the velocity interactions of the $\mathcal{V}$ morphotype; secondly collective production of extracellular 'wetting' fluid for movement; thirdly chemotactic signalling. These cell–cell communication capabilities allow regulation and control of colonies, since their stage as a whole can affect the state of the individual cells and vice versa.

8.1. *Three levels of information transfer and the concept of cybernators*

We further proposed that yet another regulation channel is required, from the level of the colony to a third level, below that of the individual cell [22, 23]. This third level is related to autonomous genetic agents (phages, plasmids, transposons, etc.) in the genome [93]. These agents, which presumably originated from viruses 'tamed' by the bacteria, can have their own 'self-interests', that is regulation of activity and replication, and their own direct communication channels to the conditions outside the cell. It is also known that such elements can perform genetic changes in the genome of the host cell. These agents are some of the main 'tools' used nowadays in genetic engineering [93]. In [22] we proposed that the genome '...can perform information analysis (about the internal and external conditions) and accordingly perform designed changes in the stored information. That is, the genome can be viewed as an adaptive cybernetic unit'. In [23] we developed this line of thought and proposed that a crucial function of the autonomous elements in the genome is to perform the cybernetic processes. As we have said: 'It is natural to expect, as is argued by Shapiro [93], that organisms use these naturally available 'tools' in the processes of adaptation and evolution. It is an evolutionary advantage to the host cell'. Thus the autonomous genetic elements may be viewed as cybernetic units, to describe their functional role. We designate as *cybernators* the cybernetic agents† whose function is regulated by colony parameters such as growth kinetics, cellular density, density variations and level of stress. The crucial point is that, since the cybernators' activity is regulated by colony parameters, it can produce changes in the genome's activity and structure that will modify the individual cells in a manner beneficial to the colony as a whole. Thus the bacteria possess a cybernetic capacity which serves to regulate three levels of interactions: the cybernator, the cell and the colony. The 'interest' of the cybernator 'serves' the 'purpose' of the

†An agent here is not necessarily a specific single macromolecule. It could be a combination of units or even a collective excitation of the genome performing the specific function. In other words, generally it should be viewed as a conceptual unit, although specifically it might be one macromolecule or a collection of molecules.

colony by readjusting the genome of the single cell. The cybernator provides a singular feedback mechanisms as the colony uses it to induce changes in the single cell, thus leading to consistent adaptive self-organization of the colony.

8.2. *Back to the concept of complexity*

The above brings us back to the concept of complexity as a means to describe evolving systems. In part I [15], I described the crucial role of microscopic–macroscopic interplay during diffusive patterning of non-living systems. In the conclusions there, I mentioned that it is tempting to introduce the concept of complexity as a quantitative measure of this interplay. Here we have seen the role of three levels interplay in determining adaptive self-organization during colonial growth. Again, it is tempting to introduce the concept of complexity as a quantitative measure of either the interplay or the resulting colonial organization. I believe that here, in the definition of complexity, may lie a bridge from azoic evolving systems to living systems. With the growing interest in evolving systems (either living or non-living) the term complexity rapidly gains popularity in many disciplines of science and engineering, with some academic centres and departments explicitly devoted to the study of complex systems [94]. Many attempts have been made to define complexity as the variable relevant for evolving systems, a variable which is the analogue of entropy in systems at equilibrium. In spite of these efforts, we still lack a commonly accepted definition of complexity and it is not clear that indeed such a real variable exists, real in the sense that a measurement of the variable can be defined. Meantime, there is much confusion and fuzziness in the way that the concept of complexity is used as defined in [95]: '**Complexity**. The quality or condition of being complex. **1**. Composite nature or structure ... **2**. Involved nature or structure, intricacy ... At least two different meanings are intermingled [96–98]. One is in the sense of spatial and/or temporal structure and organization, that is the number of elements that compose the system and their connections and organizations, which could be referred to as *configurational complexity* or *organizational complexity*. The other meaning is in the sense of how complicated it is for an observer to understand or describe the system, which could be referred to as *epistemic complexity* or *operational complexity*.

When we examine other concepts relevant to colonial developments, such as adaptation, flexibility, fitness and survival, it appears that they are also used in various meanings. Even more confusing and obscure are the relations between the different concepts. The situation reminds one of the state of affairs prior to the development of thermodynamics. New definitions of the commonly used concepts of heat, energy and temperature had to be established alongside the definition of entropy. This conceptual barrier had to be breached before the theory could be developed. Now we are facing a similar conceptual barrier which prevents the development of a theory for evolving systems.

8.3. *Back to the patterning in colonies*

I concluded part I saying: 'The next hint might be provided from the observations of complex patterning in bacterial colonies.' Now, at the end of part II, it is time to wonder whether indeed the bacteria give us insight into complexity. Clearly, our studies did not take us over the conceptual barrier, and a theory for evolving systems is yet to be developed. Neverthess I believe that they did help us construct a more firm basis for future studies. We have gained important hints which can help us to formulate more defined questions and to clarify the future research directions. For example, we realized that the two notions of complexity, both configurational and operational, play an important role in colonial development. The first has to do with the observed pattern and the second is related to the cybernetic capacity, that is to the potential to develop the complex patterning and the potential for transitions between morphotypes, each morphotype with its own ability to develop different levels of configurational complexity.

An example of the kinds of riddle posed by the bacterial colonies is demonstrated in figures 23 (*a*) and (*b*). The observed patterns look very complex. They are composed of many different geometrical elements (i.e. global twist, local twist, thin chiral branches, wide branches, wavy pattern, etc.) organized in a mixture of order and disorder. In the introduction I said that, as a general rule, we expect more complex patterns as the growth conditions become more adverse. Here we see that the situation is not that simple. The patterns in figure 23 (*a*) and (*b*) are of growth with a high level of nutrients and soft agar, namely relatively 'convenient' growth conditions. Why are, then, the emerging patterns so complex? Perhaps it is not the organizational complexity that increases with adverse growth conditions but the operational complexity.

With the communicating walkers at our disposal, we can test various quantitative definitions of the configurational complexity. I have mentioned the 'fastest-growing morphology' selection principle. Is it equivalent to selecting the more complex pattern? Or perhaps the more flexible colony? Here flexibility is defined as the variation in configurational complexity with the imposed growth conditions. These are just a few examples of the kinds of questions that we now, after the studies presented here, have the tools to study.

Figure 23. (*a*), (*b*) $\mathcal{T}$ **morphotype grown on soft agar (0.5%) for peptone levels of (a) 10 g** l^{-1} **and (b) 5 g** l^{-1}**. On such soft agar the** $\mathcal{T}$ **morphotype is transformed to** $\mathcal{C}$ **morphotype. (*c*) Result of a 'mixture' experiment. The initial inoculum consists of** $\mathcal{C}$ **morphotype with 0.1%** $\mathcal{T}$ **morphotype. The growth conditions are an agar concentration of 1% and a peptone level of 1.5 g** l^{-1}**. The initial growth is chiral followed by a tip-splitting growth from which bursts of chiral patterns are observed.**

8.4. *Comment about future directions*

I have in mind a long list of additional tasks that may now be performed. However, to avoid making these conclusions look like a research proposal, I shall describe only one additional example concerning the $\mathcal{T} \rightleftarrows \mathcal{C}$ transitions. As I mentioned in section 6, it is the colonial selection pressure and not the advantage to the individual cells of the new morphotype that leads to the transitions. Hence a finite nucleation is required for the new morphotype to be expressed. Is population dynamics

sufficient to create the finite nucleation, or perhaps genetic cotransformations and autocatalytic mutations are needed? By population dynamics I mean that there are continuous transitions from $\mathcal{T}$ bacteria to C bacteria. That is, even when we start with pure $\mathcal{T}$ inoculum, after a while the colony is a mixture of the two types, and the dynamics of growth lead to finite nucleation of C after which C will burst out.

At present, having a good understanding how to model both the $\mathcal{T}$ and the C morphotypes, we can construct a model which will enable us to study the above questions. Such a model will be an extension of the previous models including the option for each walker to mutate and change its length, thus turning into a C bacterium (in section 6 we correlate the change in length with the $\mathcal{T} \rightarrow C$). Including a finite rate of $\mathcal{T} \rightarrow C$ transitions, we can test numerically whether population dynamics are sufficient for a burst of the C morphotype. Alternatively, we can include, in the model cotransitions, autocatalytic transitions or quornum-dependent transitions and test their ability to cause finite nucleation of the bursting morphotype. We can also start, both numerically and experimentally, with a colony which is a mixture of $\mathcal{T}$ and C and observe the 'winning' of the preferred morphotype. Comparison of the numerical and experimental results will provide us with valuable new insights. In figure 23 we show experimental results of the first step in this direction. We show growth of C with 0.1% of $\mathcal{T}$ bacteria added. The agar is soft so that C is the preferred morphotype. Naively we would expect, under such conditions, that the addition of 0.1% $\mathcal{T}$ will have no effect at all. Looking at the figure, clearly the outcome is in contrast with the expectations. This picture demonstrates the kind of fascinating observations and intellectual challenges awaiting ahead. We do not understand this surprising result. We can say that it is probably a result of population dynamics, but a much more sophisticated mechanisms, waiting to be revealed and explained, leads to the observed phenomenon.

To conclude, many results have been presented. Yet we are far from the end of the story. Plenty of research is waiting ahead, whose outcomes are likely to be even more exciting than what has already been found. One of my major goals in writing this extended review was to attract researchers to join this wonderful endeavour. I hope that I have succeeded to convey both the beauty of the newly evolving field and the intellectual challenges that it presents.

Acknowledgements

I am very grateful to my student Inon Cohen for his most valuable help in the preparation of this article. The manuscript describes results obtained over few years with many collaborators. I thank J. Shapiro for his criticisms and encouragement during this time. The studies of the $\mathcal{T}$ and C morphotypes were done with I. Cohen, A. Czirók, O. Shochet, A. Tenenbaum and T. Vicsek. The first isolation of the $\mathcal{V}$ morphotype was done with O. Avidan, A. Dukler, D. L. Gutnick, O. Shochet and A. Tenenbaum. Studies of the $\mathcal{V}$ morphotype were done with I. Cohen, A. Czirók, D. L. Gutnick and T. Vicsek. Currently, the genetic nature of the various strains is being studied together with I. Cohen, E. Freidkin, D. L. Gutnick and is also being studied by R. Rudner. The original *B. subtilis* 168 strain was provided by E. Ron. The other *B. subtilis* strains were designed and provided by R. Rudner. I am grateful to I. Brainis for her technical assistance. The research was supported in part by grant No. BSF 92-00051 from the Israel USA Binational Foundation, by grant No. 593-95 from The Israeli Academy of Science and by the Siegl Prize for Research.

References

[1] Albrecht-Buehler, G., *Int. Rev. Cytol.*, **120,** 1919.
[2] Pelce, P. and Pocheau, A., 1992, Geometrical approach to the morphogenesis of unicellular algea, *J. theor. Biol.*, **156,** 197 – 214.
[3] Rosenberg, E. (editor), 1984, *Myxobacteria Development and Cell Interactions* (New York: Springer).
[4] Kessler, J. O., 1985, Co-operative and concentration phenomena of swimming micro-organisms, *Contemp. Phys.*, **26,** 147 – 166.
[5] Shapiro, J. A., 1988, Bacteria as multicellular organisms, *Sci. Am.*, **258,** 62 – 69.
[6] Haken, H., 1988, Information and self-organization., (Berlin: Springer).
[7] Nicolis, G. and Prigogine, I., 1989, *Exploring Complexity* (New York: W. H. Freeman).
[8] Shapiro, J. A. and Trubatch, D., 1991, Sequential events in bacterial colony morphogenesis, *Physica D.*, **49,** 214 – 223.
[9] Kessler, D. A. and Levine, H., 1993, Pattern formation in *Dictyostelium* via the dynamics of cooperative biological entities, *Phys. Rev. E.*, **48,** 4801 – 4804.
[10] Wiener, N., 1948, *Cybernetics: or Control and Communication in the Animal and Machine* (New York: Wiley).
[11] Doudoroff, M., Stainer, R. Y. and Adelberg, E. A., 1957, *The Microbial World* (New Jersey: Englewood Cliffs, Prentice-Hall).
[12] Kessler, D. A., Koplik, J. and Levine, H., 1988, Pattern selection in fingered growth phenomena, *Ad. Phys.*, **37,** 255.
[13] Langer, J. S., 1989, Dendrites, viscous fingering, and the theory of pattern formation, *Science*, **243,** 1150 – 1154.
[14] Ben-Jacob, E. and Garik, P., 1990, The information of patterns in non-equilibrium growth, *Nature*, **343,** 523 – 530.
[15] Ben-Jacob, E., 1993, From snowflake formation to the growth of bacterial colonies, part I: Diffusive patterning in non-living systems, *Contemp. Phys.*, **34,** 247 – 273.
[16] Mandelbrot, B. B., 1977, *Fractals: Form, Chance and Dimension* (San Francisco, California: Freeman).
[17] Mandelbrot, B. B., 1977, *The Fractal Geometry of Nature* (San Francisco, California: Freeman).
[18] Fujikawa, H. and Matsushita, M., 1989, Fractal growth of *Bacillus subtilis* on agar plates, *J. phys. Soc. Japan*, **58,** 3875 – 3878.
[19] Matsushita, M. and Fujikawa, H., 1990, Diffusion-limited growth in bacterial colony formation, *Physica A.*, **168,** 498 – 506.

[20] Matsushita, M., Wakita, J.-I. and Matsuyama, T., 1995, Growth and morphological changes of bacteria colonies, *Spatio-Temporal Patterns in Nonequilibrium Complex Systems*, Santa Fe Institute Studies in the Sciences of Complexity, edited by P. E. Cladis and P. Palffy-Muhoray (Reading, Massachussetts: Addison-Wesley), pp. 609 – 618.

[21] Ben-Jacob, E., Shochet, O., Tenenbaum, A. and Avidan, O., 1995, Evolution of complexity during growth of bacterial colonies, *Spatio-Temporal Patters in Nonequilibrium Complex Systems*, edited by P. E. Cladis and P. Palffy-Muhoray (Reading, Massachussetts: Addison-Wesley), pp. 619 – 634.

[22] Ben-Jacob, E., Shmueli, H., Shochet, O and Tenenbaum, A., 1992, Adaptive self-organization during growth of bacterial colonies, *Physica A.*, **187,** 378 – 424.

[23] Ben-Jacob, E., Tenenbaum, A., Shochet, O. and Avidan, O., 1994, Holotransformations of bacterial colonies and genome cybernetics, *Physcia A.*, **202,** 1 – 47.

[24] Ben-Jacob, E., Shochet, O. and Tenenbaum, A., 1994, Bakterien schließen sich zu bizarren formationen zusammen, *Muster des Ledendigen: Faszination inher Entstehung und Simulation*, edited by A. Deutsch (Braunschweig: Vieweg).

[25] Matsuyama, T., Harshey, R. M. and Matsushita, M., 1993, Self-similar colony morphogenesis by bacteria as the experimental model of fractal growth by a cell population, *Fractals*, **1,** 302 – 311.

[26] Matsuyama, T. and Matsushita, M., 1993, Fractal morphogenesis by a bacterial cell population, *Crit. Rev. Microbiol.*, **19,** 117 – 135.

[27] Ben-Jacob, E., Shochet, O., Tenenbaum, A., Cohen, I., Czirók, A. and Vicsek, T., 1994, Generic modelling of cooperative growth patterns in bacterial colonies, *Nature*, **368,** 46 – 49.

[28] Ben-Jacob, O., Shochet, O., Tenenbaum, A., Cohen, I., Czirók, A. and Vicsek, T., 1994, Communication, regulation and control during complex patterning of bacterial colonies, *Fractals*, **2,** 15 – 44.

[29] Ben-Jacob, E., Cohen, I., Shochet, O., Aranson, I., Levine, H. and Tsimiring, L., 1995, Complex bacterial patterns, *Nature*, **373,** 566 – 567.

[30] Ben-Jacob, E., Cohen, I., Shochet, O., Czirók, A. and Vicsek, T., 1995, Cooperative formation of chiral patterns during growth of bacterial colonies, *Phys. Rev. Lett.*, **75,** 2899 – 2902.

[31] Czirók, A., Ben-Jacob, E., Cohen, I. and Viscek, T., 1996, Formation of complex bacterial colonies via self-generated vortices, *Phys. Rev. E.*, **54,** 1791 – 1801.

[32] Ben-Jacob, E., Cohen, I., Czirók, A., Viscek, T. and Gutnick, D. L., 1997, Chemomodulation of cellular movement and collective formation of vortices by swarming bacteria and colonial development, *Physica A.* (in press).

[33] Mendelson, N. H., 1978, Helical *Bacillus subtilis* macrofibers: morphogenesis of a bacterial multicellular macroorganism, *Proc. natln. Acad. Sci. USA*, **75,** 2478 – 2482.

[34] Devreotes, P., 1989, *Dictyostelium discoideum*: a model system for cell – cell interactions in development, *Science*, **245,** 1054 – 1058.

[35] Matsuyama, T., Kaneda, K., Nakagawa, Y., Isa, K., Hara-Hotta, H. and Yano, I., 1992, A novel extracellular cyclic lipopeptide which promotes flagellum-dependent and -independent spreading growth of *Serratia marcescens*, *J. Bacteriol.*, **174,** 1769 – 1776.

[36] Harshey, R. M., 1994, Bees aren't the only ones: swarming in gram-negative bacteria, *Molec. Microbiol.*, **13,** 389 – 394.

[37] Fuqua, W. C., Winans, S. C. and Greenberg, E. P., 1994, Quorum sensing in bacteria: the luxr – luxi family of cell density-responsive transcriptional regulators, *J. Bacteriol.*, **176,** 269 – 275.

[38] Latifi, A., Winson, M. K., Foglino, M., Bycroft, B. W., Stewart, G. S., Lazdunski, A. and Williams, P., 1995, Multiple homologues of luxr and luxi control expression of virulence determinants and secondary metabolites through quorum sensing in *Pseudomonas aeruginosa* paol. *Molec. Microbiol.*, **17,** 333 – 343.

[39] Budrene, E. O. and Berg, H. C., 1991, Complex patterns formed by motile cells of *Escherichia coli*, *Nature*, **349,** 630 – 633.

[40] Blat, Y. and Eisenbach, M., 1995, Tar-dependent and -independent pattern formation by *Salmonella typhimirium*, *J. Bacterial.*, **177,** 1683 – 1691.

[41] Budrene, E. O. and Berg, H. C., 1995, Dynamics of formation of symmetrical patterns by chemotactic bacteria, *Nature*, **376,** 49 – 53.

[42] Fujikawa, H. and Matsushita, M., 1991, Bacterial fractal growth in the concentration field of nutrient, *J. phys. Soc. Japan*, **60,** 88 – 94.

[43] Ryan, F. J. and Wainwright, L. K., 1954, Nuclear segregation and the growth of clones of spontaneous mutants of bacteria, *J. Gen. Microbiol.*, **11,** 364 – 379.

[44] Shapiro, J. A., 1984, Observations on the formation of clones containing arab – lacz cistron fusions, *Molec. gen. Genet.*, **194,** 79 – 90.

[45] Cairns, J., Overbaugh, J. and Miller, S., 1988, The origin of mutants, *Nature*, **335,** 142 – 145.

[46] Hall, B. G., 1988, Adaptive evolution that requires multiple spontaneous mutations. i. mutations involving an insertion sequence, *Genetics*, **120,** 887 – 897.

[47] Hall, B. G., 1991, Adaptive evolution that requires multiple spontaneous mutations: mutations involving base substitutions, *Proc. natln. Acad. Sci. USA*, **88,** 5882 – 5886.

[48] Foster, P. L., 1993, Adaptive mutation: the uses of adversity, *A. Rev. Microbiol.*, **47,** 467 – 504.

[49] Shapiro, J. A., 1995, Adaptive mutations: who's really in the garden, *Science*, **268,** 373 – 374.

[50 Lenski, R. E., Slatkin, M. and Ayala, F. J., 1989, Mutation and selection in bacterial populations: alternatives to the hypothesis of directed mutation, *Proc. natln. Acad. Sci. USA*, **86,** 2775 – 2778.

[51] Gutnick, D., 1995, (private communication).

[52] Allison, C. and Hughes, C., 1991, Bacterial swarming: an example of prokrayotic differentiation and multicellular behavior. *Sci. Prog.*, **75,** 403 – 422.

[53] Gutnick, D. L., Freidkin, E. and Cohen, I., 1997, unpublished; Rudner, R., 1992, unpublished.

[54] Ben-Jacob, E., Garik, P., Muller, T. and Grier, D., 1988, Characterization of morphology transitions in diffusion-controlled systems, *Phys. Rev. A.*, **38,** 370.

[55] Mendelson, N. H. and Salhi, B., 1996, Patterns of reporter gene expression in the phase diagram of *Bacillus subtilis* colony forms, *J. Bacteriol.*, **178,** 1980 – 1989.

[56] Eisenbach, M., 1990, Functions of the flagellar modes of rotation in bacterial motility and chemotaxis, *Molec. Microbiol.*, **4,** 161 – 167.

[57] Henrichsen, J., 1972, Bacterial surface translocation: a survey and a classification, *Bacteriol. Rev.*, **36,** 478 – 503.

[58] Kaiser, D. and Losick, R., 1993, How and why bacteria talk to each other, *Cell*, **73,** 873 – 887.

[59] Grossman, A. D. and Losick, R., 1988, Extracellular control of spore formation in *Bacillus subtilis*, *Proc. natln. Acad. Sci. USA*, **85,** 4369 – 4373.

[60] Kuspa, A., Plamann, L. and Kaiser, D., 1992, A-signalling and the cell density requirement for *Myxococcus xanthus* development, *J. Bacteriol.*, **174,** 7360 – 7369.

[61] Adler, J., 1969, Chemoreceptors in bacteria, *Science*, **166,** 1588 – 1597.

[62] Berg, H. C. and Purcell, E. M., 1977, Physics of chemoreception, *Biophys. J.*, **20,** 193 – 219.

[63] Lackiie, J. M., (editor), 1986, *Biology of the Chemotactic Response* (Cambridge University Press).

[64] Berg, H. C., 1993, *Random Walks in Biology* (Princeton University Press).

[65] Murray, J. D., 1989, *Mathematical Biology* (Berlin: Springer).

[66] Adler, J., 1966, Chemotaxis in bacteria, *Science*, **153,** 708 – 716.

[67] Wolfe, A. J. and Berg, H. C., 1989, Migration of bacteria in semisolid agar, *Proc. natln. Acad. Sci. USA*, **86,** 6973 – 6977.

[68] Horgan, J., 1995, From complexity to perplexity, *Sci. Am.*, **95,** 74 – 79.

[69] Azbel, M. Y., 1993, Survival – extinction transition in bacteria growth, *Europhys. Lett.*, **22,** 311 – 316.

[70] Shochet, O., Kassner, K., Ben-Jacob, E., Lipson, S. G. and MÜller-Krumbhaar, H., 1992, Morphology transition during non-equilibrium growth: I study of equilibrium shapes and properties, *Physica A.*, **181,** 136 – 155.

[71] Shochet, O., Kassner, K., Ben-Jacob, E., Lipson, S. G. and Müller-Krumbhaar, H., 1992, Morphology transition during non-equilibrium growth: II. morphology diagram and characterization of the transition, *Physica A.*, **187,** 87 – 111.

[72] Shochet, O., 1995, Study of late-stage growth and morphology selection during diffusive patterning, PhD thesis, Tel-Aviv University.

[73] Tsimiring, L., Levine, H., Aranson, I., Ben-Jacob, E., Cohen, I., Shochet, O. and Reynolds, W. N., 1995, Aggregation patterns in stressed bacteria, *Phys. Rev. Lett.*, **75,** 1859 – 1862.

[74] Ben-Jacob, E., Shochet, O., Tenenbaum, A., Cohen, I., Czirók, A. and Vicsek, T., 1996, Response of bacterial colonies to imposed anisotropy, *Phys. Rev. E.*, **53,** 1835 – 1845.

[75] Hegstrom, R. A. and Kondepudi, D. K., 1990, The handedness of the universe, *Sci. Am.*, **262,** 108 – 115.

[76] Avetisov, V. A., Goldanskii, V. I. and Kuzmin, V. V., 1991, Handedness, origin of life and evolution, *Phys. Today*, July, 33 – 41.

[77] Mendelson, N. H. and Keener, S. L., 1982, Clockwise and counter-clockwise pinwheel colony morphologies of *Bacillus subtilis* are correlated with the helix band of the strain, *J. Bacteriol.*, **151,** 455 – 457.

[78] Mendelson, N. H. and Thwaites, J. J., 1989, Cell wall mechanical properties as measured with bacterial thread made from *Bacillus subtilis*, *J. Bacteriol.*, **171,** 1055 – 1062.

[79] Mendelson, N. H., 1990, Bacterial macrofibres: the morphogenesis of complex multicellular bacterial forms, *Sci. Prog.*, **74,** 425 – 441.

[80] Stock, J. B., Stock, A. M. and Mottonen, M., 1990, Signal transduction in bacteria, *Nature*, **344,** 395 – 400.

[81] Shaw, C. H., 1991, Swimming against the tide: chemotaxis in *Agrobacterium*, *BioEssays*, **13,** 25 – 29.

[82] Ford, W. W., 1916, Studies on aerobic spore-bearing non-phatogenic bacteria. part ii. Miscellaneous cultures, *J. Bacteriol.*, **1,** 518 – 526.

[83] Smith, R. N. and Clacrk, F. E., 1938, Motile colonies of *Bacillus alvei* and other bacteria, *J. Bacteriol.*, **35,** 59 – 60.

[84] Wolf, G. (editor), 1968, *Encyclopaedia Cinematographica* (Göttagen: Institut für Wissenschaftlichen Film).

[85] Reynolds, C. W., 1987, Flocks, herds, and schools: a distributed behavioral model, *Comput. Graphics*, **21,** 25 – 34.

[86] Toner, J. and Tu, Y., 1995, Long-range order in a two-dimensional dynamical *xy* model: how birds fly together, *Phys. Rev. Lett.*, **75,** 4326 – 4329.

[87] Dukler, A., 1993, Isolation and characterization of bacteria growing in patterns on the surface of solid agar, Senior project under the supervision of D. Gutnick, Tel-Aviv University.

[88] Hemmingsson, J., 1995, Modellization of self-propelling particles with a coupled map lattice model, *J. Phys. A.*, **28,** 4245 – 4250.

[89] Duparcmeur, Y. L., Herrmann, H. and Troadec, J. P., 1995, Spontaneous formation of vortex in a system of self motorized particles, *J. Phys. Paris I.*, **5,** 1119 – 1128.

[90] Ben-Jacob, E., Cohen, I. and Czirók, A., 1996, Smart bacterial colonies, *Physics of Biological Systems: From Molecule to Species*, Edited by H. Flyvbgerg, J. H. Mogens, H. Jensen, O. G. Movritsen and K. Sneppen. (Berlin: Springer). 307 – 324.

[91] Ben-Jacob, E. and Cohen, I., 1997, Cooperative formation of bacterial patterns, *Bacteria as Multicellular Organisms*, edited by J. A. Shapiro and M. Dwarkin (Oxford University Press) 394 – 416.

[92] Shapiro, J. A. and Dwarkin, M., (editors), 1997, *Bacteria as Multicellular Organisms,* pp. 394 – 416.

[93] Shapiro, J. A., 1992, Natural genetic engineering in evolution, *Genetica*, **86,** 99 – 111.

[94] Waldrop, M. M., 1992, *Complexity: The Emerging Science at the Edge of Order and Chaos* (New York: Simon & Schuster).

[95] Simpson, J. A. and Weiner, E. S. C. (editors), 1989, *The Oxford English Dictionary*, Vol. III, second edition (Oxford University Press).

[96] Atlan, H., 1974, On a formal definition of organization, *J. Theor. Biol.*, **45,** 295 – 304.

[97] Atlan, H., 1987, Self-creation of meaning, *Phys. Scripta*, **36,** 563 – 576.

[98] Atlan, H., 1989, Natural complexity and self-creation of meaning, *Mind over Matter: Symposium in Honour of Professor Bernhard Witkop* (Jerusalem: Israel Academy of Sciences and Humanities).